NASA/TM—2012-217613

Analysis of 100-lb_f (445-N) LO_2-LCH_4 Reaction Control Engine Impulse Bit Performance

William M. Marshall and Julie E. Kleinhenz
Glenn Research Center, Cleveland, Ohio

June 2012

NASA STI Program . . . in Prof le

Since its founding, NASA has been dedicated to the advancement of aeronautics and space science. The NASA Scientif c and Technical Information (STI) program plays a key part in helping NASA maintain this important role.

The NASA STI Program operates under the auspices of the Agency Chief Information Off cer. It collects, organizes, provides for archiving, and disseminates NASA's STI. The NASA STI program provides access to the NASA Aeronautics and Space Database and its public interface, the NASA Technical Reports Server, thus providing one of the largest collections of aeronautical and space science STI in the world. Results are published in both non-NASA channels and by NASA in the NASA STI Report Series, which includes the following report types:

- TECHNICAL PUBLICATION. Reports of completed research or a major signif cant phase of research that present the results of NASA programs and include extensive data or theoretical analysis. Includes compilations of signif cant scientif c and technical data and information deemed to be of continuing reference value. NASA counterpart of peer-reviewed formal professional papers but has less stringent limitations on manuscript length and extent of graphic presentations.

- TECHNICAL MEMORANDUM. Scientif c and technical f ndings that are preliminary or of specialized interest, e.g., quick release reports, working papers, and bibliographies that contain minimal annotation. Does not contain extensive analysis.

- CONTRACTOR REPORT. Scientif c and technical f ndings by NASA-sponsored contractors and grantees.

- CONFERENCE PUBLICATION. Collected papers from scientif c and technical conferences, symposia, seminars, or other meetings sponsored or cosponsored by NASA.

- SPECIAL PUBLICATION. Scientif c, technical, or historical information from NASA programs, projects, and missions, often concerned with subjects having substantial public interest.

- TECHNICAL TRANSLATION. English-language translations of foreign scientif c and technical material pertinent to NASA's mission.

Specialized services also include creating custom thesauri, building customized databases, organizing and publishing research results.

For more information about the NASA STI program, see the following:

- Access the NASA STI program home page at *http://www.sti.nasa.gov*

- E-mail your question to *help@sti.nasa.gov*

- Fax your question to the NASA STI Information Desk at 443–757–5803

- Phone the NASA STI Information Desk at 443–757–5802

- Write to:
  STI Information Desk
  NASA Center for AeroSpace Information
  7115 Standard Drive
  Hanover, MD 21076–1320

NASA/TM—2012-217613

Analysis of 100-lb_f (445-N) LO_2-LCH_4 Reaction Control Engine Impulse Bit Performance

William M. Marshall and Julie E. Kleinhenz
Glenn Research Center, Cleveland, Ohio

National Aeronautics and
Space Administration

Glenn Research Center
Cleveland, Ohio 44135

June 2012

Acknowledgments

The authors greatly acknowledge the entire facilities team which operated the Altitude Combustion Stand (ACS) facility and made testing possible. Additionally, the support received by the NASA Glenn Materials Branch is also appreciated, as well as discussion and insight provided by the engine manufacturer, Aerojet. This work was supported by the Propulsion and Cryogenic Advanced Development (PCAD) project, which was part of the NASA Exploration and Technology Development Program (ETDP).

Level of Review: This material has been technically reviewed by technical management.

Available from

NASA Center for Aerospace Information
7115 Standard Drive
Hanover, MD 21076–1320

National Technical Information Service
5301 Shawnee Road
Alexandria, VA 22312

Available electronically at http://www.sti.nasa.gov

Contents

Analysis of 100-lb_f (445-N) LO_2-LCH_4 Reaction Control Engine Impulse Bit Performance

William M. Marshall and Julie E. Kleinhenz
National Aeronautics and Space Administration
Glenn Research Center
Cleveland, Ohio 44135

Summary

Recently, liquid oxygen-liquid methane (LO_2-LCH_4) has been considered as a potential "green" propellant alternative for future exploration missions. The Propulsion and Cryogenic Advanced Development (PCAD) project was tasked by NASA to develop this propulsion combination to enable safe and cost-effective exploration missions. To date, limited experience with such combinations exist, and as a result a comprehensive test program is critical to demonstrating with the viability of implementing such a system. The NASA Glenn Research Center conducted a test program of a 100-lb_f (445-N) reaction control engine (RCE) at the Center's Altitude Combustion Stand (ACS), focusing on altitude testing over a wide variety of operational conditions. The ACS facility includes unique propellant conditioning feed systems (PCFS), which allow precise control of propellant inlet conditions to the engine. Engine performance as a result of these inlet conditions was examined extensively during the test program. This paper is a companion to the previous specific impulse testing paper, and discusses the pulsed-mode operation portion of testing, with a focus on minimum impulse bit (MIB) and repeatable pulse performance. The engine successfully demonstrated target MIB performance at all conditions, as well as successful demonstration of repeatable pulse widths. Some anomalous conditions experienced during testing are also discussed, including a double pulse phenomenon, which was not noted in previous test programs for this engine.

1.0 Introduction

To enable future exploration of the Moon, Mars, and beyond, next-generation propellant systems are being developed. With an emphasis on nontoxic, "green" propellants, liquid oxygen-liquid methane (LO_2-LCH_4) has risen to the forefront. LCH_4 is an attractive propellant because it does not require the strict thermal storage requirements of hydrogen (due to its larger density and higher boiling point), nor does it require the rigorous handling protocols of toxic hypergolic propellants. It also has the potential, when paired with LO_2, to produce higher specific impulse than either the existing hypergolic or LO_2-kerosene systems. This higher specific impulse and improved storage capability could reduce vehicle mass when compared with hydrogen-based systems, since smaller propellant storage and management would be required. Not only is there a potential for decreased vehicle mass, these propellants can also be produced on Mars using local resources. Prior work with this propellant combination is limited, so a goal of the NASA Propulsion and Cryogenic Advanced Development (PCAD) project was to examine the feasibility and performance characteristics of these systems (Refs. 1 to 3). In particular, there is interest in demonstrating repeatable and reliable ignition of an engine over a wide range of valve inlet temperatures (from liquid-liquid operation to gas-gas operation), especially at vacuum conditions (Refs. 3 and 4).
To facilitate this, a 100-lb_f (445-N) LO_2-LCH_4 Reaction Control Engine (RCE) was developed by Aerojet Corporation (Ref. 5). In late 2009 and 2010, this engine underwent a series of tests in the Altitude Combustion Stand (ACS) at the NASA Glenn Research Center (Refs. 6 and 7). Two specially designed Propellant Conditioning Feed Systems (PCFS) were developed to enable precise propellant temperature control. The first test series (Refs. 6 and 7) at ACS examined specific impulse performance with burn durations up to 7 s. The engine met the $I_{sp,vac}$ goal, achieving an overall average $I_{sp,vac}$ of 305 s, ±4 percent.

Performance improved as propellant temperature increased or mixture ratio (*MR*) decreased, which is believed to be a result of injection and mixing effects (Ref. 7).

Since this type of engine is more likely to operate in a pulsed operation, the next test series focused on impulse bit (I-bit) performance. Propellant inlet temperatures were again varied to the same three target conditions used in the specific impulse tests: (1) Cold (170 °R (94.4 K) LCH_4, 163 °R (90.5 K) LO_2), (2) Nominal (204 °R (113 K)) and (3) Warm (224 °R (124 K)). Mixture ratio was maintained at 2.5, which is the nominal operating condition. The goals were to prove repeatable ignition and performance, with a target I-bit of 4 lb_f-s, a minimum pulse duration of 80 ms, and operation at a variety of duty cycle conditions. The results of these tests will be discussed here.

2.0 NASA Glenn Altitude Combustion Stand Facility

Altitude testing of the RCE was conducted in the NASA Glenn ACS facility. This facility was originally part of the NASA Glenn (then NASA Lewis) Rocket Engine Test Facility (RETF) (B-Stand) (Refs. 8 to 10). The current capabilities of this facility are described in Reference 7. A photograph of the spray cart and test capsule of the ACS facility is shown in Figure 1.

Data acquisition is achieved through a National Instruments module (Ref. 11) and timing is controlled by a programmable logic controller (PLC). The module allows for real-time, streaming views of data at nominal sample rates of up to 1000 Hz and multiple computers in the control room allow for quick-view (post-test) processing, providing researchers vital information to rapidly adjust test conditions and prepare for the next test.

Figure 1: ACS facility test capsule, spray cart, and ejector platform.

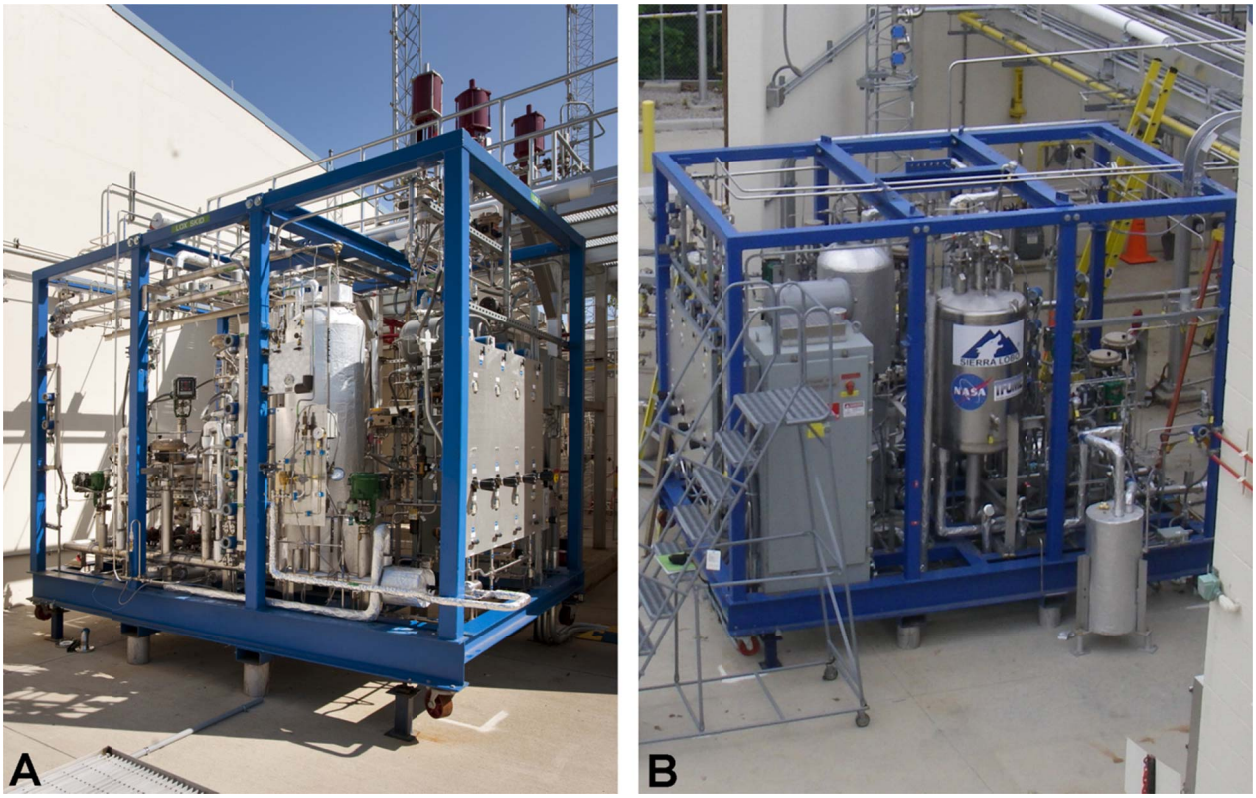

Figure 2: Propellant Conditioning Feed System (PCFS) outside of Altitude Combustion Stand (ACS) at NASA Glenn. (A) Liquid oxygen, LO_2. (B) Liquid methane, LCH_4.

3.0 Propellant Conditioning Feed System (PCFS)

For the current investigation, performance and characterization of the RCE under pulsed-mode operation at various propellant inlet temperatures was the primary interest. To accomplish this, propellant conditioning feed systems (PCFS) were incorporated into the facility for control of propellant conditions. One system was dedicated to methane conditioning, while the other was dedicated to oxygen conditioning. Both have been described in detail previously (Refs. 6, 7, 12, and 13). The systems were designed to condition each of the propellants to ±5 °R (±2.8 K). Photographs of the LO_2 and LCH_4 systems located outside of ACS are shown in Figure 2.

4.0 Hardware Description

The test article for this test series was the Aerojet-designed 100-lb_f (445-N) RCE thruster (Refs. 5 to 7 and 14). This engine is designed to operate at a steady-state mean chamber pressure of 175 psia (1.2 MPa) and a nominal *MR* of 2.5. Details of the engine have been described previously (Refs. 6 and 7). Only the exciter source and the operating procedures were changed for these pulse tests. A photograph of the engine with the altitude nozzle is shown in Figure 3. A photograph of the engine operating in the ACS facility is shown in Figure 4.

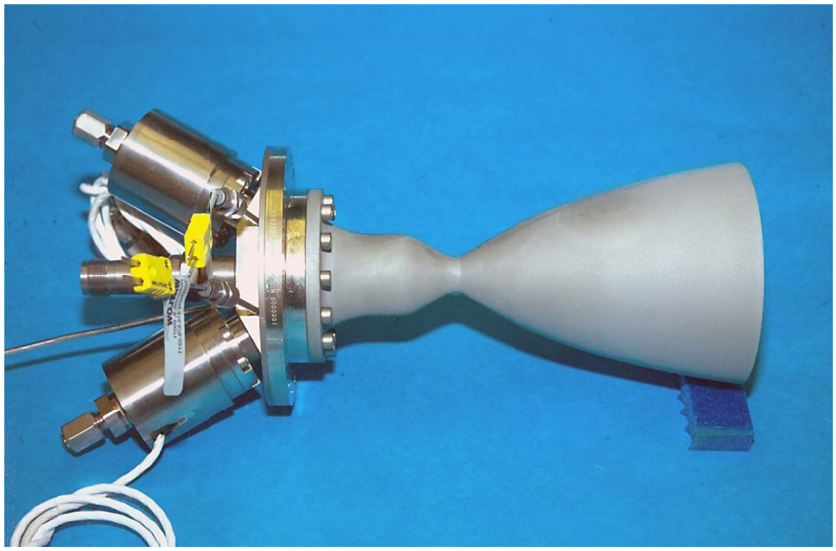

Figure 3: Photograph of the 100-lb_f (445-N) RCE with altitude nozzle.

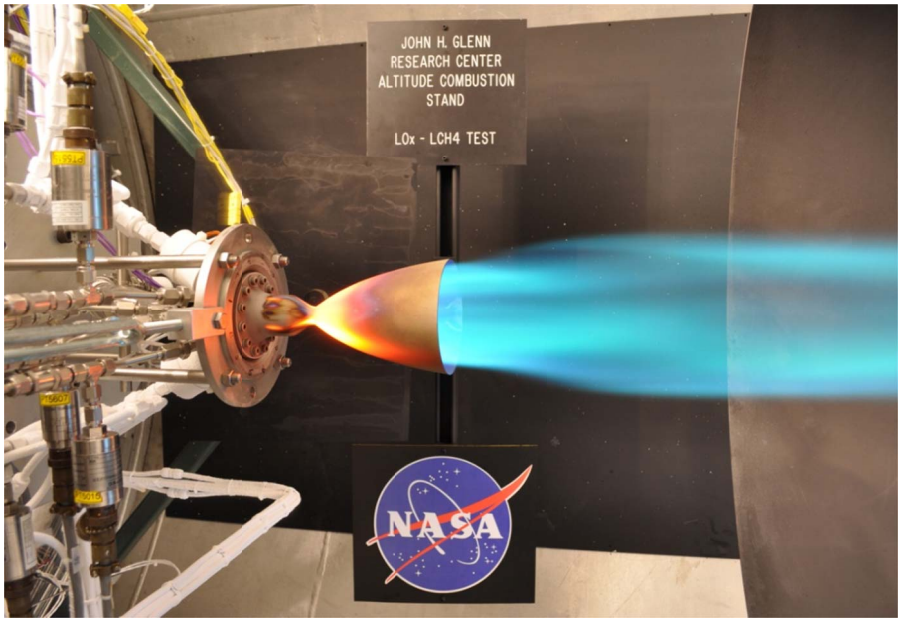

Figure 4: A 100-lb_f (445-N) LO_2-LCH_4 RCE operating in NASA Glenn Altitude Combustion Stand (ACS) test capsule.

4.1 Exciter Sources

The ignition source for the RCE was a spark torch igniter. For initial pulse testing, a Champion (Champion Aerospace, LLC) exciter was used with a spark plug igniter system. This exciter was used in the previous $I_{sp,vac}$ test program. However, due to concerns about similarities between the current test series and previous test series (Refs. 5 and 6) (see Section 6.4.5), this exciter was replaced with a similar spark exciter developed by Unison (Unison, LLC) which provided a greater spark rate. The Champion exciter was a single channel design, with a 26- to 30-V_{DC} input voltage, 94-mJ stored energy, 20-kV output ionization voltage specified, with 100 sparks per second. The Unison exciter was a single channel design, with a 23- to 36-V_{DC} input voltage, 160-mJ stored energy, 13-kV output ionization voltage

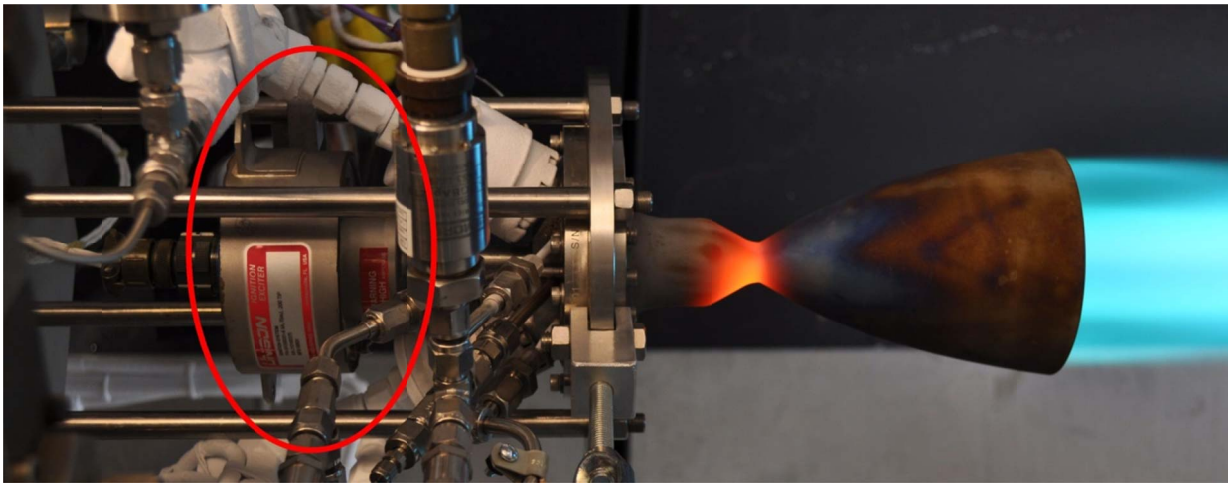

Figure 5: A 100-lb_f (445-N) RCE operating with Unison compact exciter (circled).

specified, with 200 sparks per second. At the end of the test series, a compact exciter designed by Unison was also briefly tested. The compact exciter was similar electrically to the Unison exciter, but eliminated the need of an electrical lead between the exciter unit and the spark plug. This compact exciter was a single channel design with a 23- to 36-V_{DC} input voltage, 55-mJ stored energy, and 20-kV output ionization voltage specified, with 200 sparks per second. A photograph of the engine operating with the compact exciter is shown in Figure 5.

4.2 Injector

The injector of the RCE engine was an impinging style with fuel film cooling (FFC) and an integrated igniter. Approximately 15 percent of the fuel flow is used for the FFC. The injector was designed to operate at an overall *MR* of 2.48. Surrounding the injector is a series of acoustical cavities. Chamber pressure, P_{cav}, is measured within one of these cavities.

4.3 Columbium Chamber

The combustion chamber and nozzle used for altitude testing was a single piece, radiatively cooled design, made from columbium (niobium) material and coated with an R512E oxidation resistant coating (Hitemco). For all tests described here, the nozzle throat was 0.615 in. (15.6-mm) in diameter with a 6:1 contraction ratio, 45:1 exit ratio (80 percent bell), and 2.50 in. (63.5 mm) *L′*. The chamber (nozzle) was designed to be bolted to the injector assembly. Since the chamber and nozzles are a single piece, the terms nozzle and chamber are used interchangeably throughout this paper.

4.4 Instrumentation

Figure 6 shows a schematic of the propellant feed system for the RCE engine with associated sensor locations. Unless otherwise noted, all pressure transducers were diaphragm-type transducers with a range of 0 to 500 psi (0 to 3.44 MPa). Temperature measurements deemed critical to flow measurement were made by Class-A resistance temperature detectors (RTDs), to improve precision, and all other temperature measurements were made by either K-type or T-type thermocouples. All instrumentation was sampled at 1000 Hz. In addition to the instrumentation shown, a K-type thermocouple was added into the $P_{c,ign}$ port (hereafter referred to as TC_{ign}) to help diagnose ignition phenomenon in the igniter portion of the injector, observed in the prior test series (Ref. 7). A temperature rise measured by this thermocouple would indicate warmer gases were in the igniter cavity and hence a probable ignition. Likewise, if no temperature rise or a temperature decrease was observed in this thermocouple data, it would indicate a probable non-ignition event.

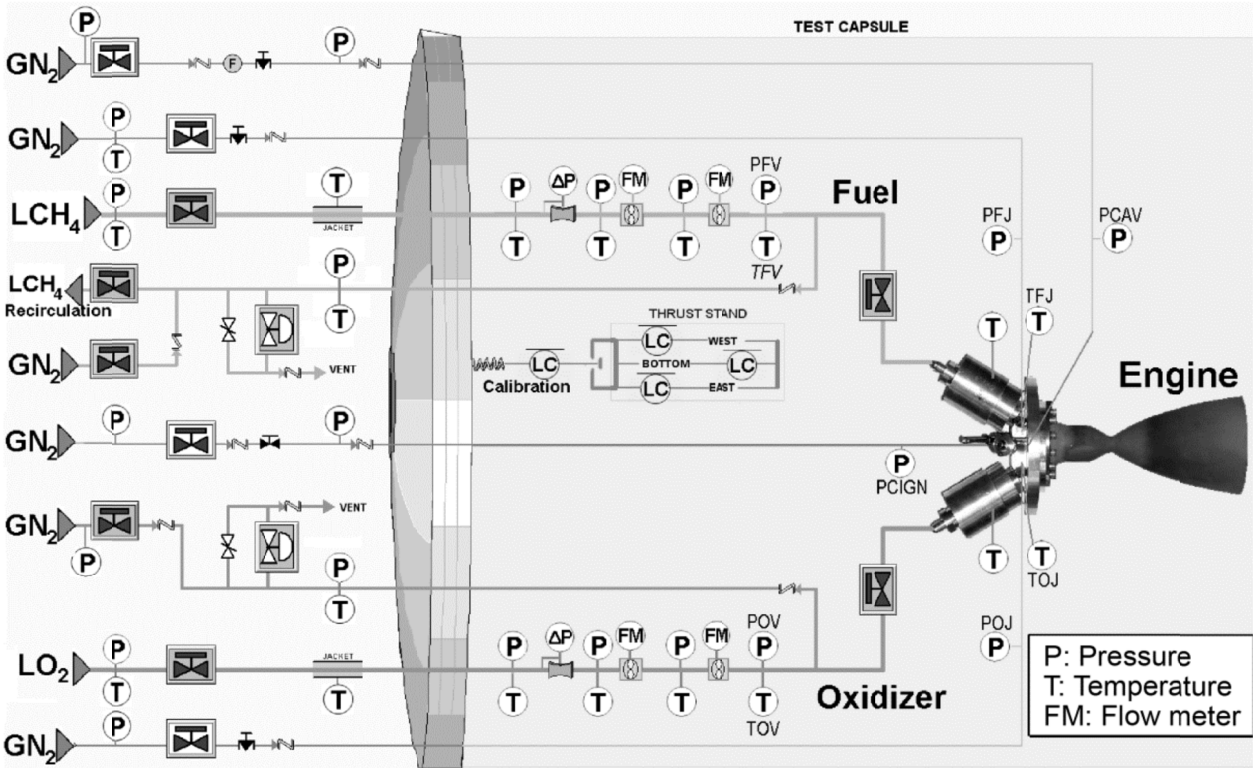

Figure 6: Feed system schematic for RCE tests in NASA Glenn Altitude Combustion Stand (ACS) facility.

4.4.1 Mass Flow Rates

Flow rate measurements were calculated using subsonic venturi, with pressure and temperature instruments immediately upstream of the venturi for fluid properties (e.g., density) determination. Fluid densities were calculated using the National Institute of Standards and Technology (NIST) REFPROP program (Ref. 15). A stainless steel 0.100-in. (2.54-mm) throat diameter venturi was used for the LO_2 leg, and a 0.080-in. (2.03-mm) throat diameter venturi was used for the LCH_4 leg. A 0- to 100-psi (0- to 0.68-MPa) differential pressure transducer was used to measure the differential pressures generated across the venturi. The venturi discharge coefficients (C_d) were measured prior to testing using nitrogen gas for the 0.100-in. (2.54-mm) venturi and liquid water for the 0.080-in. (2.03-mm) venturi. Efforts to calibrate the venturi at cryogenic conditions were not made at this time. Equation (1) lists the equation used for the sub-sonic venturi mass flow rate calculations,

$$\dot{m} = AC_d\sqrt{2\rho\Delta P} \tag{1}$$

where A is the venturi throat area (corrected for thermal contraction), C_d is the venturi discharge coefficient, ρ is the fluid density, and ΔP is the differential pressure measured across the venturi throat.

Pairs of dual-rotor turbine flow meters were also installed in series downstream of each venturi (as shown in Figure 6). Each turbine flow meter also had pressure and temperature instrumentation just upstream in order to accurately describe fluid properties entering the meter. Equation (2) is the equation used to calculate mass flow rate through the turbine flow meters,

$$\dot{m} = \rho Q \tag{2}$$

where Q is the volumetric flow rate measured by the turbine flow meter and ρ is the fluid density.

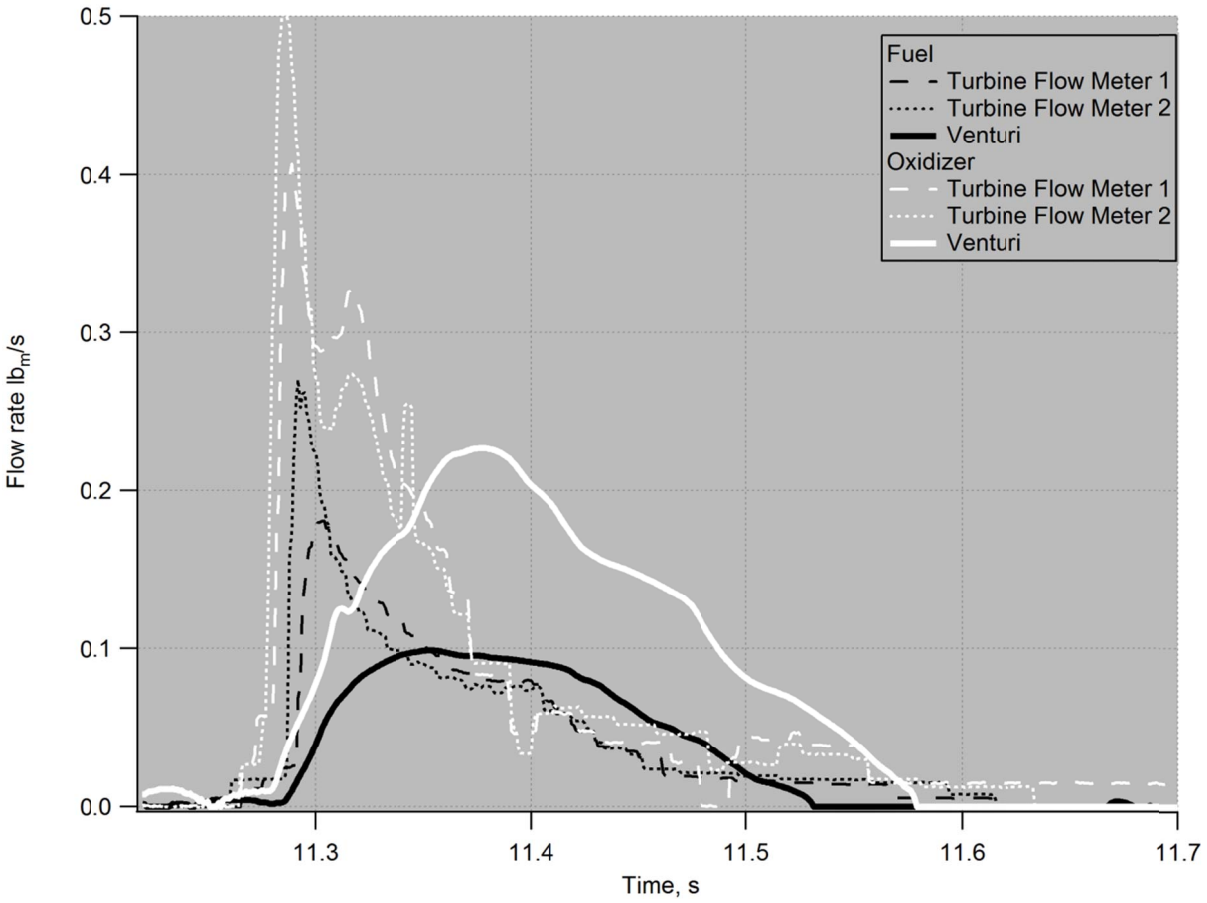

Figure 7: Flow meter measurements for a single 80-ms pulse illustrating the difference between the venturi flow meter and the turbine flow meter responses.

It was noted from previous testing that the turbine flow meters showed good agreement with the venturi flow meters under steady-state conditions. However, transient response of both instruments during the short pulse widths made it difficult to accurately determine or adjust mass flow rates. Figure 7 shows the flow rate measurements from the different flow meters, illustrating the distinctly different transient behavior for the short pulse widths. The turbine flow meters have a very sharp rise at the beginning of the pulse that then decayed down, while the venturi flow meters showed a more smoothed peak throughout the pulse. Therefore, test conditions were based upon steady-state set points, and the flow rates and *MR*s were permitted to vary based upon the transient behavior of the engine feed system. The reported flow rates are time average values over the pulse duration based upon the venturi flow meter measurements.

4.4.2 Thrust Measurement

The thrust stand utilized a tri-load cell configuration. The total thrust was the summation of these three load cell measurements, after appropriate zero offsets were applied. Each load cell was a dual bridge design with a 0- to 100-lb_f (0- to 445-N) range (for a total thrust range of 0- to 300-lb_f (0- to 1334-N)).

Calibration of the load cells was accomplished by performing a test pull on the live bed prior to testing, but after the propellant lines and associated hardware had been chilled down in the vacuum chamber (by introducing cryogenics up to the thruster valves). This minimized thrust errors due to thermal flexure of the thrust stand. The test pull then provided a calibration factor (K-factor), which was applied to the summed load to calibrate the test thrust measurements. A final test pull at the end of the day verified the thrust stand calibration did not significantly drift throughout the test day.

4.5 Timing and Permissives

In order to ensure proper conditions are met for safe and controlled tests in ACS, two different checks are conducted. The first checks are system permissives. These are conditions that must be met prior to a test and include "rig-ready" signals from the PCFS, proper power and electrical conditions to the test cell, and proper supply pressure for system pressurants. Once the permissives are met, operators are then permitted by the PLC to start a test. Timing for a test at ACS is handled in four zones, which are described in Reference 7. Unless otherwise noted, only Zone 2, the hot fire portion, is discussed in this document. In order to achieve pulse testing, the command timing of Zone 2 encompassed a single pulse. This zone was then repeated to achieve the desired number of consecutive pulses. The timing of a pulse included a 10-ms LO_2 lead on startup, which was intended to bring both manifolds up to pressure at the same time based on cold propellant flow tests. A 5-psia (0.03-MPa) nitrogen gas purge was introduced through the igniter cavity pressure port ($P_{c,ign}$) and manifold pressure ports (PFJ and POJ) between pulses using a check valve. This purge ensured that no combustible gas was trapped in the manifolds between pulses, minimizing the chances for a hard start. The igniter sparks were initiated 20 ms before the LCH_4 flow. Table I lists the command timing with respect to the zone start, and the duration that the valve remains in that commanded state. Thus, a valve (or abort window) that opens at 30 ms with a duration of 50 ms would mean the valve opened at 30 ms into zone 2 and closed at 80 ms into zone 2. The minimum timing resolution of the PLC was 10 ms. The implications of this timing schedule are discussed in Section 4.7.1 below. At the end of the pulse, the LO_2 valve was closed with the LCH_4 following 40 ms later. This fuel- rich shutdown was intended to prevent oxidation on the hot chamber walls.

No attempt was made for a "pre-chill" (pre-flow of LO_2 to lower the injector hardware temperature) of the engine prior to start of test. However, the propellant lines were maintained at chilled conditions up to the thruster valves during and between runs by means of trace cooling around the propellant lines. Since no pre-chill was conducted, the injector often started at near ambient temperature (≈500 °R (278 K)). Therefore, there was a considerable transient on startup as the liquid propellant phase changes to gas phase in the manifolds and the manifolds subsequently chill-in.

The electric pulse width (EPW) is the time when both thruster valves are commanded open. In the current study, this is between the opening of the methane valve and when the oxygen valve closes. The duty cycle is the EPW divided by the total run time for a single pulse. Thus, for 80-ms EPW with a 5-percent duty cycle, the dwell time between pulse starts would be 1600 ms (1.6 s). Figure 8 shows a basic timing sequence used for these series of tests. Unless otherwise noted, this timing was maintained for all tests described here.

TABLE I: TIMING FOR VARIOUS PULSE WIDTHS (EPWs) USED IN PULSE TESTING

EPW, ms	Zone 2,[a] ms (% duty cycle)	Spark on/duration, ms	Oxygen on/duration, ms	Fuel on/duration, ms	P_{cav} abort window start/duration, ms
500	980 (50)	230/100	240/500	250/510	350/300
100	380 (25)	30/100	40/110	50/140	120/20
80	1580 (5)	30/90	40/90	50/120	120/10
40	780 (5)	30/60	40/50	50/80	OFF

[a]Zone 2 is repeated for desired number of pulses. Zone 2 is left 20 ms short to account for programmable logic controller (PLC) delay in repeating the zone.

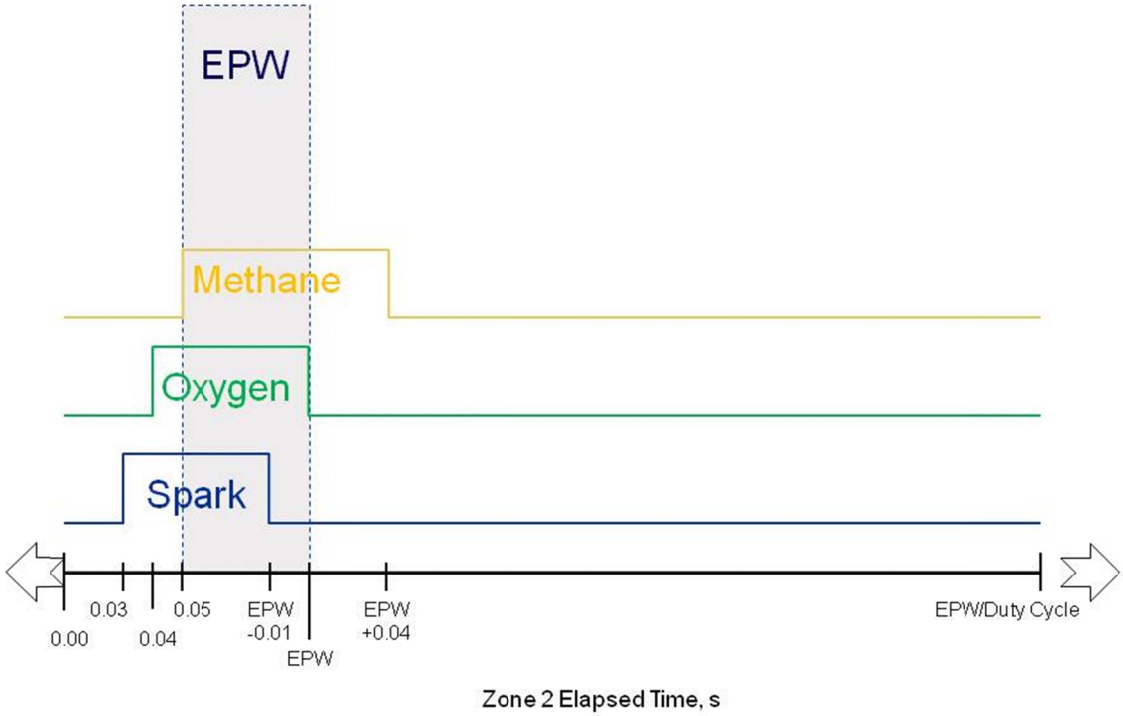

Figure 8: Basic timing sequence for individual pulses for pulse tests. EPW refers to electronic pulse width. A pulse train is accomplished by repeating the above sequence for the given number of pulses.

TABLE II: PLANNED TEST MATRIX OF INLET TEMPERATURES, °R (K)

Condition	Propellant	
	LCH_4	LO_2
Cold	170 (94)	163 (90)
Nominal	204 (113)	204 (113)
Warm	224 (124)	224 (124)

4.6 Test Matrix

For the pulse test series, the interest was testing the engine over the same matrix of temperature conditions explored in the prior duration testing. Table II lists the propellant target temperatures. Figure 9 shows the planned target temperature ranges (boxes) with the actual conditions shown. In Figure 9, the small shaded boxes are the target conditions, the larger open boxes are the modified target conditions as discussed in Reference 7.

4.7 Hardware Issues During the Test Series

During the test series, some issues were identified that were not directly related to the test engine (RCE) but which contributed to the quality of data collected and ability to meet test objectives. These included difficulty in resolving very short EPW and the inability to reach the target cold temperatures for LCH_4.

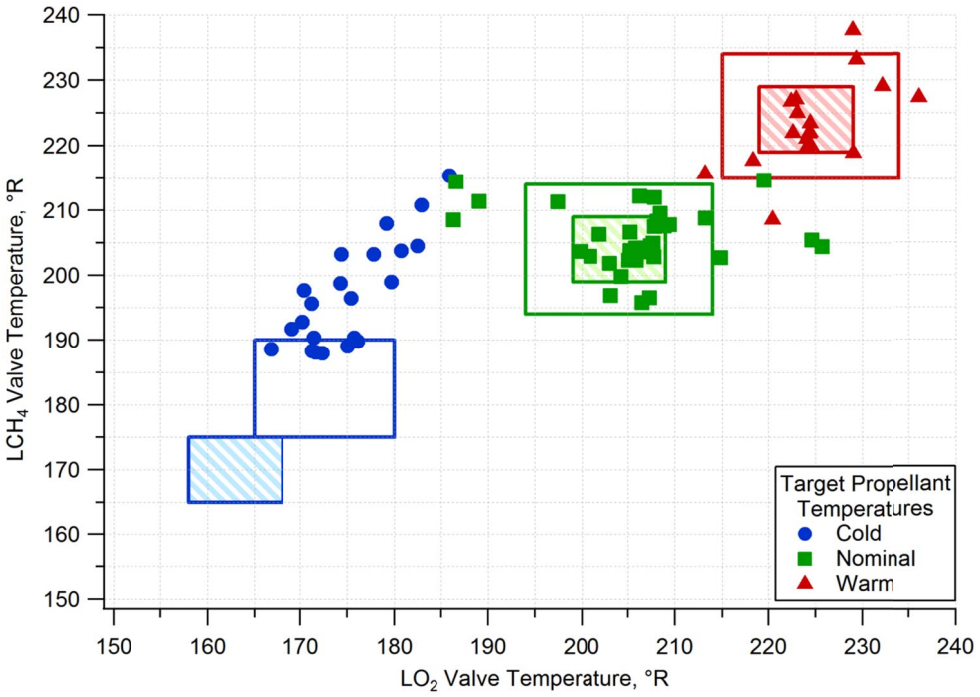

Figure 9: Propellant temperatures at the thruster valve for all tests. The boxes show target conditions based upon the planned test matrix.

4.7.1 Restricted Abort Windows and Ignition Delay

The timing resolution of the ACS facility PLC was limited to 10 ms, including abort window monitoring. The PLC checks to make sure that pressure is above a specified value throughout the duration of the window. For 80-ms EPW tests and shorter, the period of time that the chamber was sufficiently above cold flow pressures was relatively short, on the order of 10 to 40 ms. However, it was noted during previous testing (Ref. 7), and confirmed during the present series, that ignition delays of 10 to 40 ms could occur, especially at colder propellant temperatures. Figure 10 shows a plot taken during specific impulse testing (Ref. 7) illustrating observed ignition delay. During pulse testing, these delays could occur on a random pulse in a planned pulse train. A delayed ignition, due to the short abort window, would prevent chamber pressure from rising above the abort limits prior to the window end. Subsequently, shifting the abort later would cause the abort to be tripped on the shutdown for non-delayed ignitions. As a result of the restricted abort windows and the possibility of ignition delay, several pulse trains aborted during the test series. These aborts were not ignition failures, as the evidence from the data does indicate a successful ignition, but rather were a consequence of the above considerations.

4.7.2 Inoperative Methane Recirculation Pump

During the later portion (Run 224 to end of series) of the testing, the methane recirculation pump on the methane PCFS became inoperative. As a result, the capability to recirculate the methane propellant for further temperature refinement was lost, and only a single pass for temperature conditioning was possible. This particularly impacted testing at cold-cold conditions. Efforts to further condition the propellants by increasing trace cooling bleeds, etc., were employed to the extent feasible while trying to maximize the number of tests to be conducted. Figure 9 shows the plot of valve temperatures for the pulse testing program. Note that due to loss of the methane recirculation pump, methane temperatures for cold conditions were actually closer to nominal conditions.

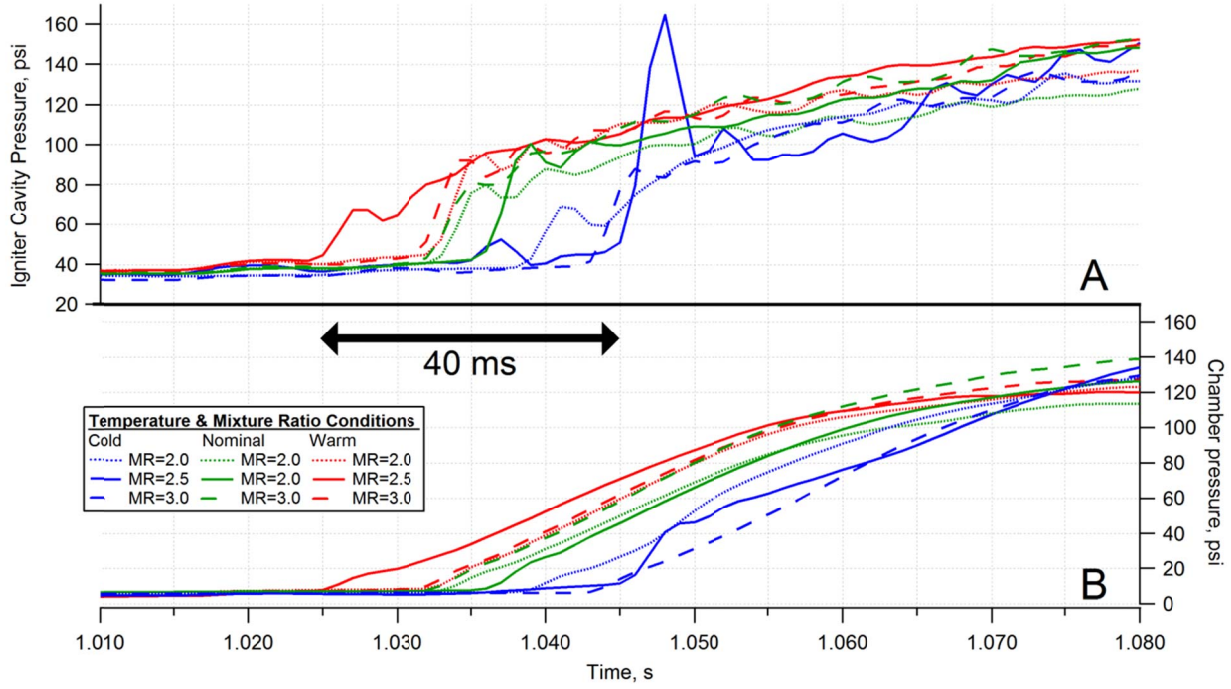

Figure 10: Ignition delay during I_{sp} testing as observed in the (A) igniter chamber pressure and (B) main chamber pressure.

5.0 Methodology

In this section, the primary performance metric for this test program, I-bit, will be defined. The major objectives of the test series are also discussed.

5.1 Definition and Calculation of Impulse Bit (I-bit)

I-bit is defined as the area under the vacuum thrust curve from the time both propellant valves open until the chamber pressure decays to 10 percent of the rated nominal chamber pressure (17.5 psia (0.12 MPa) for the RCE, which has a 175-psia (1.2-MPa) nominal chamber pressure). This definition is consistent with Aerojet's calculations from previous testing (Ref. 5).

Data from each test was imported into Microsoft Excel, where I-bit calculations were performed in a visual basic program. Figure 11 shows graphically how I-bit was calculated. The I-bit integration time was determined by examining the methane manifold pressure and the chamber pressure data sets. A pressure rise in the methane manifold indicated that both valves were open and propellants were actively flowing (Figure 11(A)). Since the end of the integration occurred during the chamber pressure decay, the peak chamber pressure was first identified. When the pressure reached 17.5 psia (0.12 MPa) (10 percent of the nominal rated value) after this peak, the integration ended (Figure 11(B)). The vacuum thrust (Figure 11(C)) was therefore integrated over this period, as represented by the gray box. The result is the I-bit, in the units of lb_f-s (N-s).

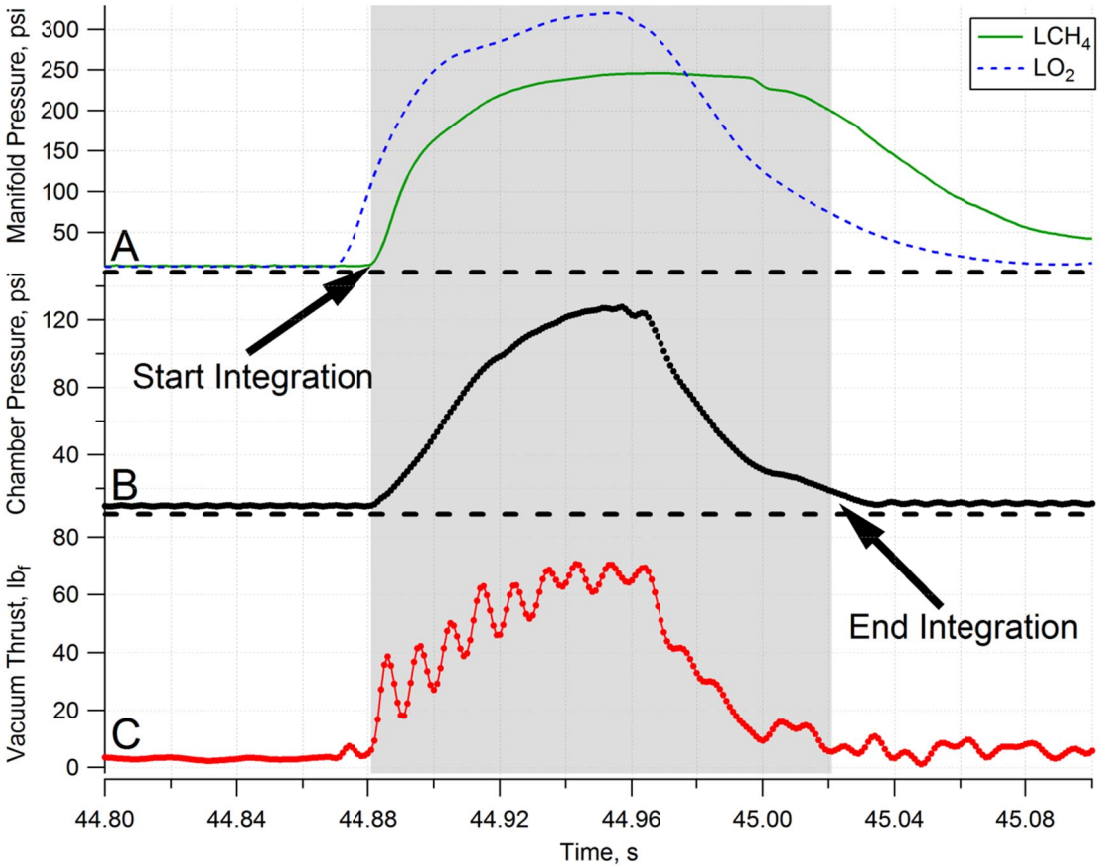

Figure 11: Calculation regime for determining I-bit.

5.2 Objectives of Pulse Testing

The objective of pulse testing at NASA Glenn was to verify the operation of the engine under a pulsed-mode operation and to quantify the I-bit performance at altitude conditions for varying input propellant temperatures. The following technical challenges had to be addressed by the delivered engine (Ref. 5).

(1) Achieve a minimum impulse bit (MIB) of 4 lb_f-s (17.8 N-s)
(2) Achieve a minimum EPW of 80 ms or less
(3) Achieve a MIB repeatability of ±5 percent after achieving stable temperature
(4) Operate over a 0- to 100-percent duty cycle

6.0 Results

Presentation of the results begins with a discussion of the uncertainty analysis utilized with an explanation of the expected uncertainties. A thorough discussion of results is then provided, concluding with a discussion of anomalies observed during the test campaign.

6.1 Uncertainty Analysis of I-bit

An uncertainty analysis was performed to qualify the I-bit values to fully meet Joint Army, Navy, NASA, Air Force (JANNAF) reporting standards (Ref. 16). The equations for I-bit and its uncertainty ($U_{\text{I-bit}}$) are

$$\text{I - bit} = \int_{\text{CH}_4\text{valve}}^{10\%P_{\text{cav}}\ \text{high}} F_{\text{vac}}\,\mathrm{d}t \tag{3}$$

$$U_{I\text{-}bit}^2 = \theta_F^2 B_F^2 + \theta_F^2 \mathcal{P}_F^2 + \theta_t^2 B_t^2 \tag{4}$$

In equation (3), F_{vac} is the vacuum thrust and t is the time. The thrust is integrated over the pulse width, as described above. In equation (4), B is the bias uncertainty that includes the instrumentation and calibration uncertainties, while $\mathcal{P}_F$ is the precision uncertainty, which represents scatter in the data. Both also include a Student's t-distribution factor for a 95-percent confidence interval, and will be discussed in more depth below. The θ values are the sensitivity terms, which are the partial derivatives of I-bit with respect to its dependent variables (F, t). Simply they are $\theta_F = t$ and $\theta_t = F$.

The bias uncertainty of time, B_t, is assumed to be negligible. The time stamp in the data files is taken from the data system clock. The bias uncertainty of the force term, $B_{F_{\text{vac}}}$, is derived from the vacuum thrust equation:

$$F_{\text{vac}} = K\left[\sum_{\substack{3\,\text{load}\\ \text{cells}}} F + P_{\text{amb}} A_e\right] \tag{5}$$

$$B_{F_{\text{vac}}}^2 = \theta_F^2 B_F^2 + \theta_K^2 B_K^2 + \theta_{P_{\text{amb}}}^2 B_{P_{\text{amb}}}^2 + \theta_{A_e}^2 B_{A_e}^2 = K^2 B_F^2 + F^2 B_K^2 + A_e^2 B_{P_{\text{amb}}}^2 + P_{\text{amb}}^2 B_{A_e}^2 \tag{6}$$

Where F is the force measured by the load cells, P_{amb} is the pressure outside the chamber, A_e is the exit area of the nozzle, and K is the calibration factor (calibrations are done at the beginning and end of each test day). The bias values were determined in the previous test program and are displayed in Table III. The previous program encompassed 55 tests, so the Student's t-distribution factor was 2 with a 95-percent confidence interval. The only term in Table III that would change with the current pulse test program is the sensitivity of the load cell calibration factor (K-factor), θ_K. As shown in Equation (6), this term is equal to the average force exerted on the load cells over all tests. For the previous program (Ref. 7) it was ≈100 lb_f (445 N) and for the pulse program it was ≈50 lb_f (222 N) in each pulse. Using the latter would decrease the bias error, $B_{F_{\text{vac}}}^2$, to a value of approximately 13.3. However, the uncertainty calculations were programmed prior to the pulse test program so estimates could be obtained in real time. Therefore, while the values in Table III are somewhat conservative, they were retained.

TABLE III: THE BIAS UNCERTAINTY FOR THE VACUUM THRUST MEASUREMENTS

	Sensitivity	b_{inst}	B_{cali}	$B^2 = \Theta^2\,\Sigma(tb)^2$
Force (summation of three load cells)	$1.033 = \theta_F$	±1 lb_f each	±0.06 lb_f each	12.862
Force calibration term (K factor)	$99.863 = \theta_K$	------	0.005	0.999
Thrust—area, exit	$0.210 = \theta_A$	±0.001 in.^2	------	1.757×10^{-7}
Thrust—pressure ambient	$13.710 = \theta_P$	±0.015 psi	0.0063	0.204
$B_{F_{\text{vac}}}^2$				14.065

The precision uncertainty, $\mathcal{P}_F$, is typically based on the standard deviation. However, the thrust is not steady in these short (80-ms) pulse durations, resulting in a bell-shaped curve over time. There is also a great deal of ringing seen in the thrust data (see Section 6.4.1). Using a simple average thrust value in the standard deviation calculation is not representative, since it neglects this time dependency. Therefore, a polynomial curve fit was used to predict a smooth, time-dependent thrust response for each pulse. The standard error of the predicted values was used to determine the precision uncertainty. Figure 12 shows thrust data and the curve fit for two pulses during a pulse train with warm propellant conditions. Ringing in the load cell causes significant fluctuations in the thrust, resulting in significant uncertainty values. Figure 12(A) was the worst in this particular train with high-amplitude fluctuations (≈40 to 100 lb_f (178 to 445 N), peak-to-peak). This resulted in a poor curve fit and high error values. Thus, the total uncertainty of the I-bit was high. In Figure 12(B) the amplitude of the thrust fluctuations were lower (≈20 to 40 lb_f (89 to 178 N), peak-to-peak), so the standard error and the resulting I-bit uncertainty were also lower. The I-bit uncertainties for each pulse are shown in Figure 13 for a representative test at each temperature condition. A 95-percent confidence interval is used to calculate the Student's *t*-distribution. The nominal propellant run has the lowest uncertainties because the thrust fluctuations tended to dampen in the tailing portion of the curve. However the I-bit uncertainty is still 30 percent even at its best. If the confidence interval is relaxed to 90 percent the uncertainties reduce to 20 percent, as represented by the dashed line for the nominal data in Figure 13.

Note that the transient nature of the short pulse durations is the primary factor in these uncertainties. Since the chamber pressure profile should trend the same as thrust, it was substituted into the I-bit equation. Without the oscillations on the thrust stand, the resulting "P_c-bit" should have a lower uncertainty than its thrust-based counterpart. However, the improvement was only a 5- to 10-percent reduction in uncertainty. The polynomial curve fit used here to estimate the precision uncertainty is not an optimal prediction of the transient effects. The bias uncertainty, which is time independent, is typically 8.5 percent on I-bit and 3.5 percent on P_c-bit. These are conservative uncertainties, but are a more accurate representation of the facility capabilities.

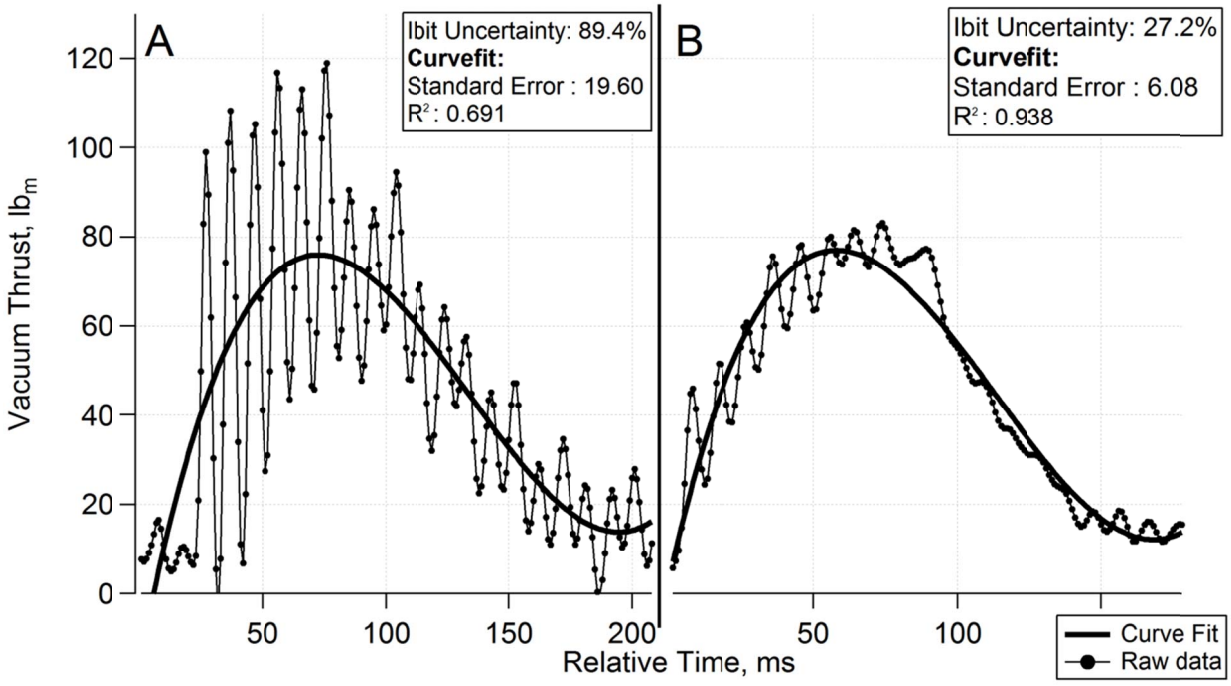

Figure 12: Thrust curves for two pulses from a test at warm propellant conditions. The solid line indicates the polynomial curve fit used to estimate the thrust precision uncertainty for (A) worst case and (B) best case thrust fluctuations.

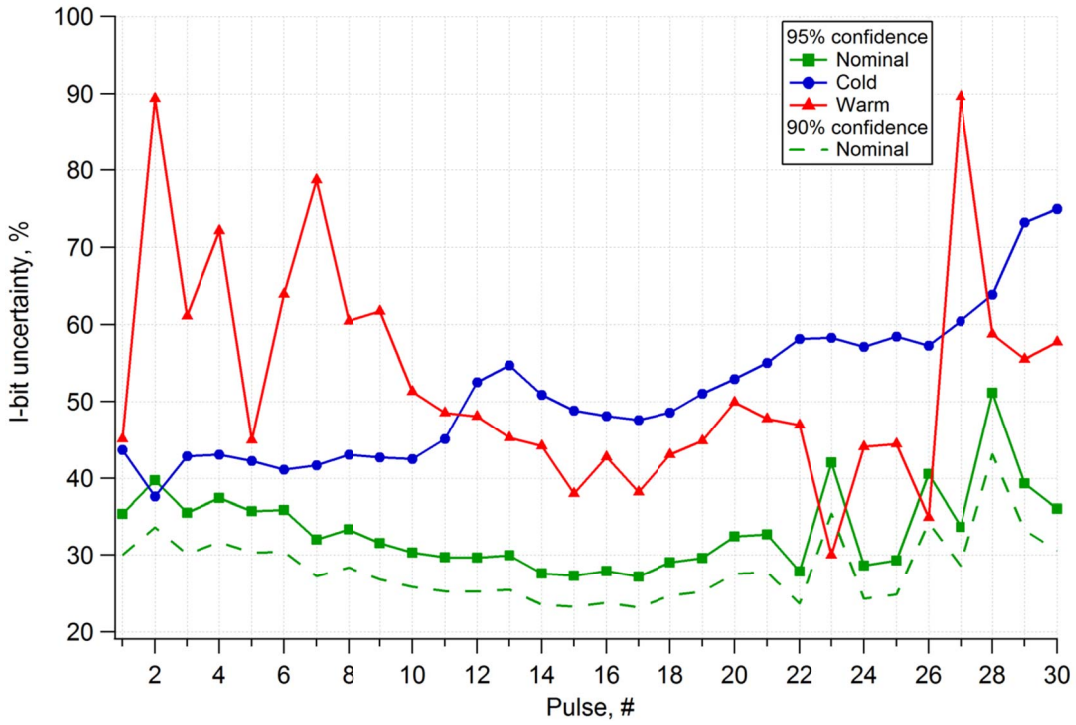

Figure 13: I-bit uncertainty for the pulse trains using a 95-percent confidence band. The dashed line shows uncertainty using a 90-percent confidence band for the nominal temperature run.

6.2 Impulse Bit Testing Results

A total of 81 tests were conducted during the pulse test series. Of those 81 tests, only four resulted in a non-ignition event, as confirmed by a lack of temperature rise observed in igniter cavity (TC_{ign}). No conclusive reason for the non-ignitions was evident from the flow conditions or data, as individual spark data (discharge voltage or current, spark pulses, etc.) was not available during this test series. As a result, it was not possible to definitively diagnose the condition of spark energy being delivered to the flow. Further investigation of ignition and spark behavior is planned in a future test series.
With respect to the major objectives of the test series, Table IV shows a table of the tested conditions with respect to pulse width (EPW) and duty cycle. The chart shows that the engine has been extensively tested over a wide variety of pulse widths and duty cycles, illustrating that it can operate over the range of duty cycles from 0 to 100 percent, as defined in objective (4) (see Section 5.2 above).

The focus of Glenn testing was minimum I-bit performance, so narrow EPWs and shorter duty cycles were used in the majority of the tests. Testing originally started at a 50-percent duty cycle, but was changed to a 25-percent and then a 5-percent duty cycle after some coating degradation was observed on the columbium chamber. It is unclear whether the duty cycle was a definitive cause of the degradation, but a low duty cycle was retained to match previous sea-level testing by Aerojet (Ref. 5). Further discussion of the coating degradation is given in Section 6.4.5. However, no correlation was observed between duty cycle and performance, as shown in Figure 14.

Since there was a programmatic requirement for a minimum EPW of 80 ms, the majority of testing at Glenn focused on this EPW, although wider and narrower pulse widths were tested. Prior testing by Aerojet (Ref. 5) showed that an EPW of 40 ms was required to reach the minimum I-bit (MIB) goal of 4 lb_f-s (17.8 N-s). Since this required the ACS facility aborts to be turned off, only a limited number of pulses were conducted at the 40-ms pulse widths. Fewer pulses would limit the amount of unburned

TABLE IV: EXAMINED ELECTRONIC PULSE WIDTH (EPW)
AND DUTY CYCLE COMBINATIONS
(AEROJET [SEA-LEVEL] = X; NASA GLENN = O; BOTH = ⊗)

EPW, ms	Duty cycle, percent							
	5	10	15	25	50	60	75	90
40	⊗		X	X				
50			X	X				
60	X		X	X		X		
80	⊗	X	X	⊗				
100	X		X	O	O			
120	X							
160	X	X	X	X				
320	X		X	X				
500					O			
960				X	X		X	X
1000				X	O			

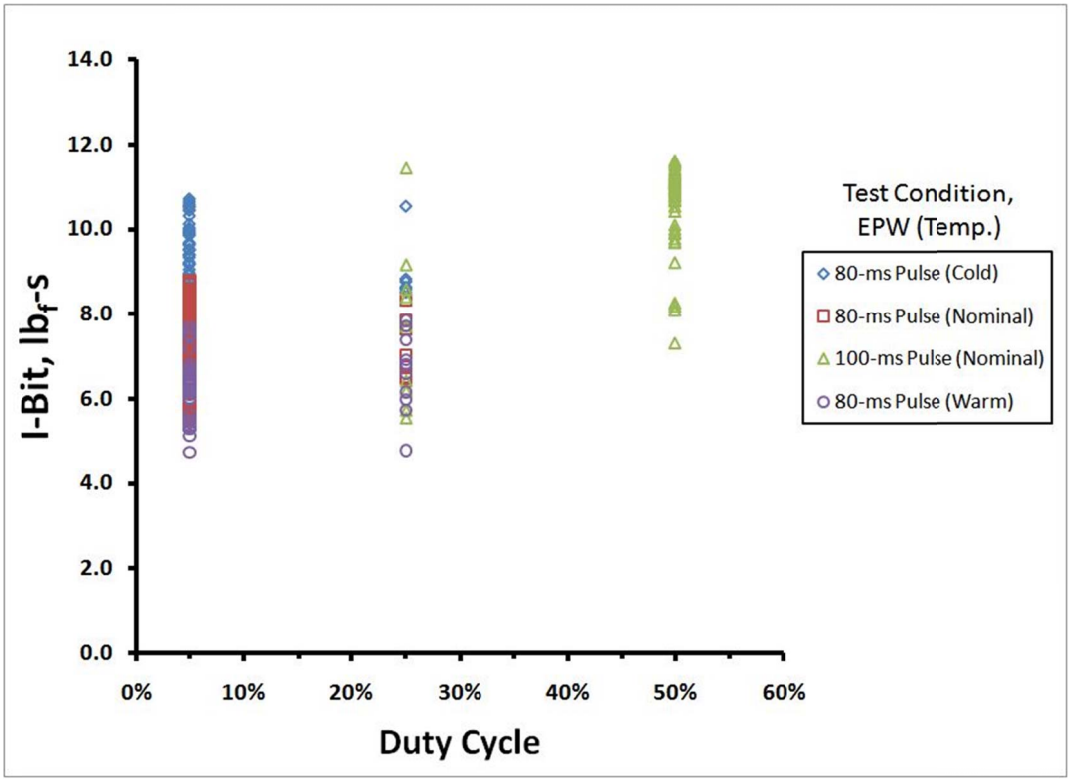

Figure 14: Plot of I-bit versus duty cycle.

methane that could build up in the test capsule in the event of a non-ignition. Figure 15 shows a plot of vacuum I-bit versus pulse number for 80-ms EPW tests. The symbols are color-coded based on propellant temperature at the LO_2 (A) and LCH_4 (B) valve inlets. There is a dependency of I-bit on valve inlet temperature, with colder propellants having higher I-bits. Figure 16 also demonstrates this observation for tests that consisted of 30 pulses. The trend shows that increasing propellant inlet temperature decreases I-bit. This is opposite of the trends observed in specific impulse testing, where increasing temperature led to increases in specific impulse and efficiency (Refs. 6 and 7).

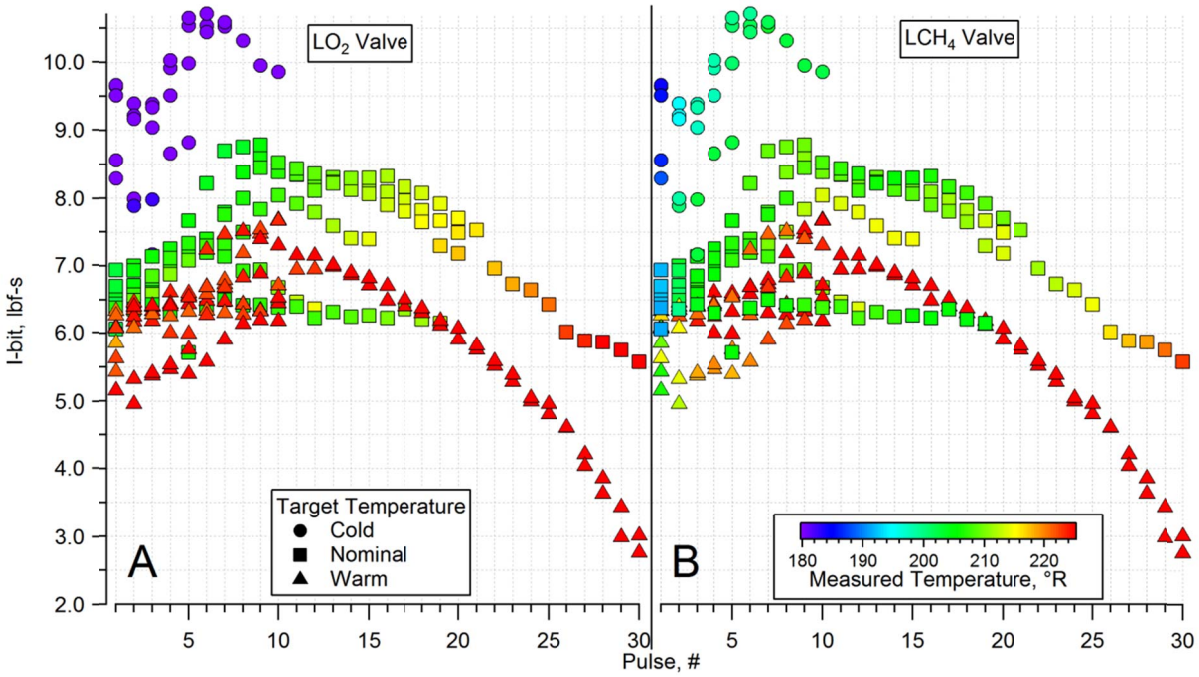

Figure 15: I-bit for each pulse with propellant inlet temperature at the (A) LO_2 and (B) LCH_4 thruster valves. Only 80-ms EPW runs with first pulse temperatures with ±10 °R of the target are shown.

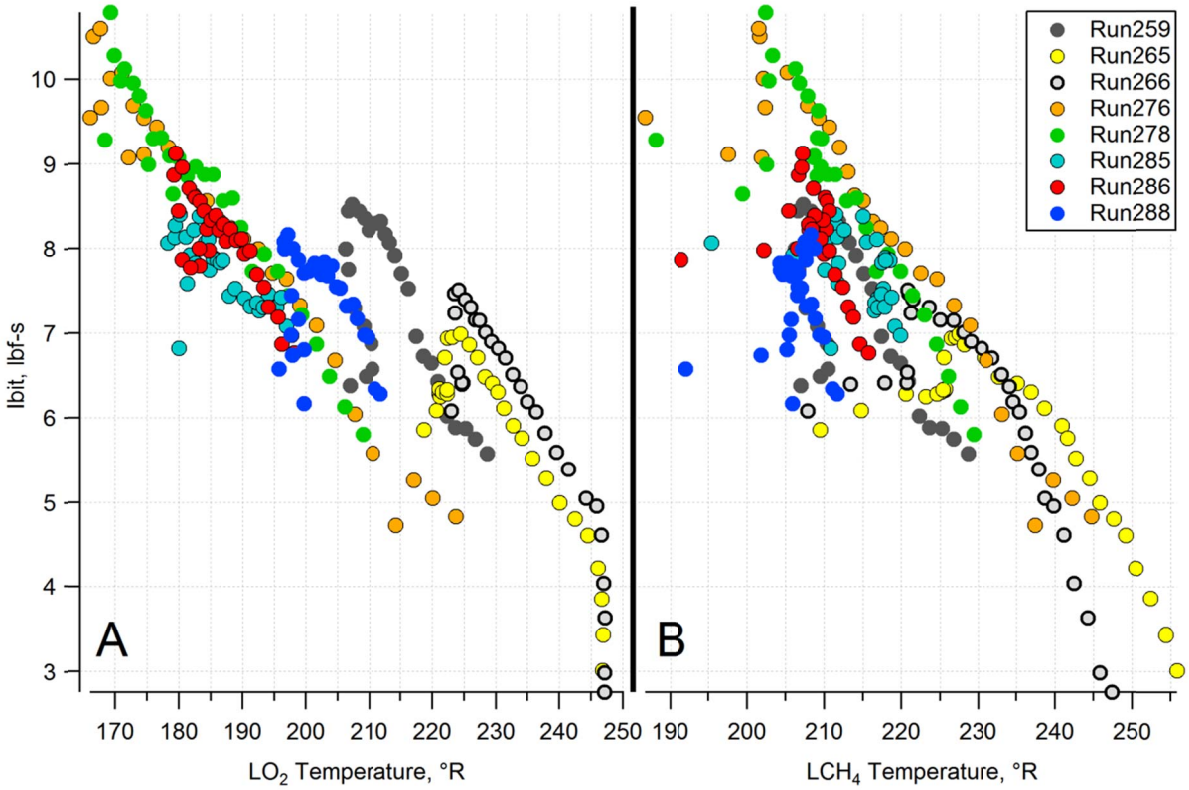

Figure 16: I-bit as a function of (A) LO_2 and (B) LCH_4 inlet temperature for 30 pulse tests.

Two factors, however, play a role in determining I-bit: (1) integration time and (2) integration of thrust, both of which may be influenced by propellant temperature. Figure 17 is a plot of integration time (a) and peak thrust (b) versus the LO_2 valve inlet temperature. Integration time is highest with colder propellants, resulting in a higher I-bit. The corresponding colder hardware temperatures may lead to trapped liquid in the manifold, which would continue to vaporize after valve closure. Thus, chamber pressure takes longer to decay, which can be seen in Figure 18. This effect is also believed to cause a "double pulse" phenomena in some tests, which will be discussed in Section 6.4.3. Thrust, shown in Figure 17(B), has a similar trend as integration time. Due to the thrust stand ringing, these peak thrust values were based upon the curve fit profile described in Section 6.1 (see Figure 12). While a trend exists, it should be noted that the majority of the peak thrust data falls within a ±10- to 15-lb_f (±45- to 67-N) band, while oscillations observed in the thrust stand were as great as ±40 to 100 lb_f (±178 to 445 N), peak-to-peak. Thus, it is difficult to claim a significant contribution to I-bit based upon thrust, and the cause of the I-bit trend can be primarily attributed to integration time. It should also be noted that average, nominal temperature I-bit values were consistent with values previously reported in Aerojet testing (Ref. 5), suggesting I-bit calculation methods are consistent.

With an EPW of 40 ms, the engine could achieve the MIB requirement of 4 lb_f-s (17.8 N-s) consistently, for a variety of propellant inlet temperatures. Figure 19 shows a plot of 40-ms EPW tests with the data points color mapped to propellant inlet temperatures. From the previously observed 80-ms EPW tests, warm tests generally have lower I-bit than cold tests. Thus, it is not clear why a single warm data run shows such a significantly larger I-bit (≈40 percent) than colder tests at otherwise similar conditions. This set of data clearly defies trends observed, and is considered here as a statistical outlier. All of the other 40-ms EPW runs demonstrate a MIB of 4 lb_f-s (17.8 N-s) or less, which is consistent with prior Aerojet testing (Ref. 5).

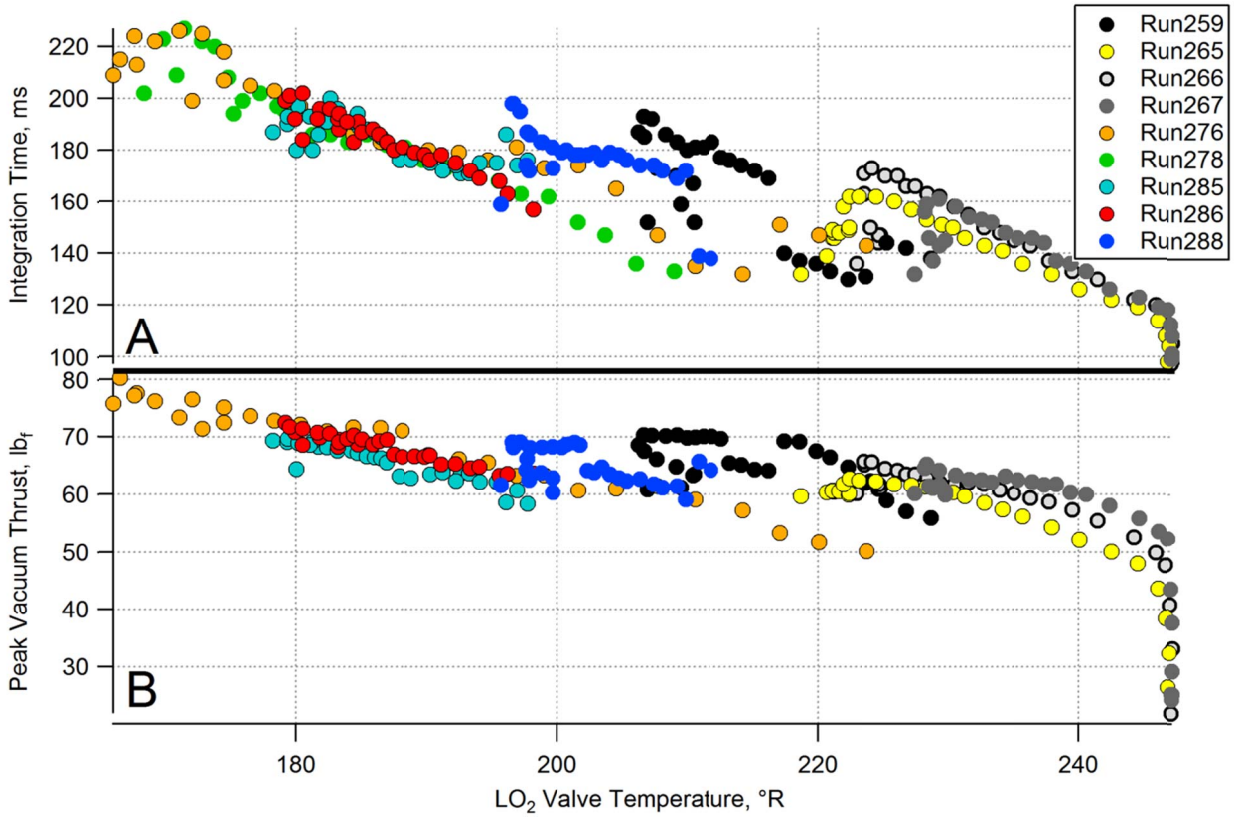

Figure 17: The effect of LO_2 inlet temperature on (A) integration time and (B) peak thrust.

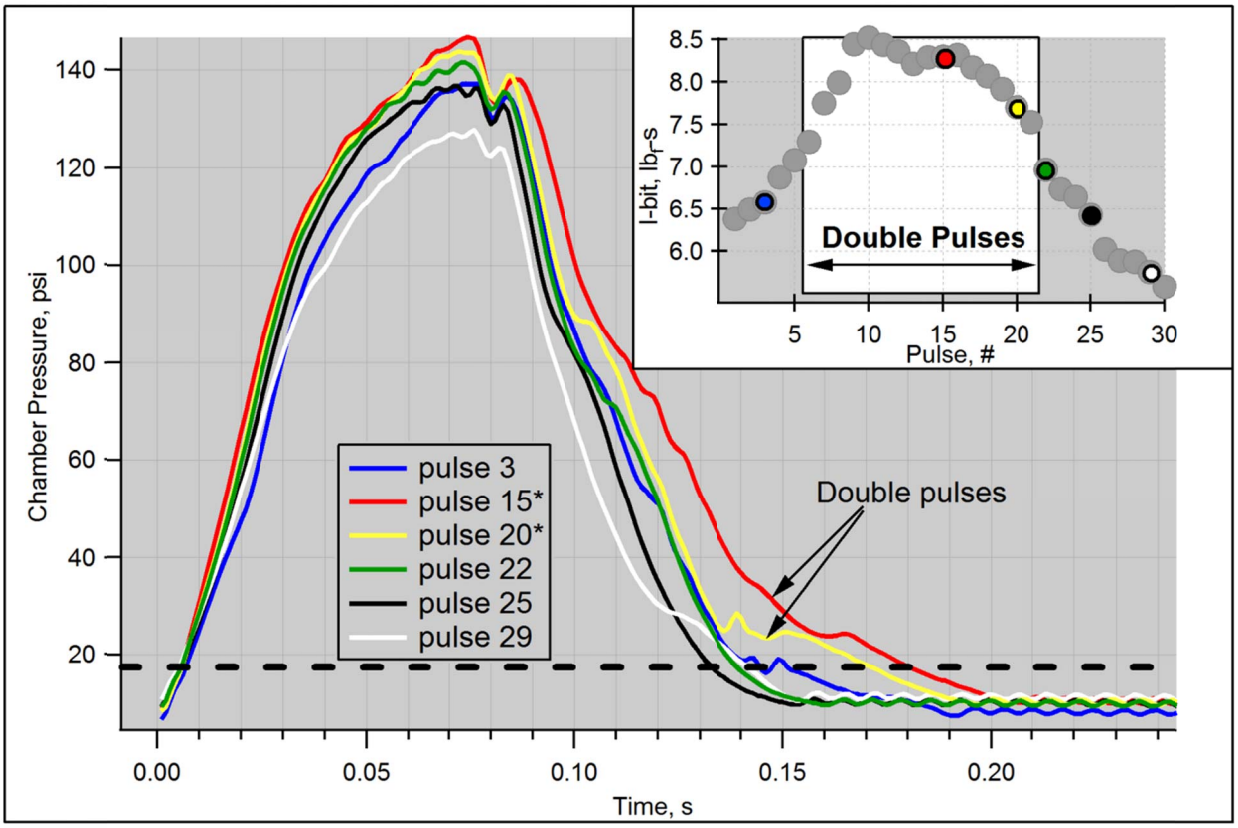

Figure 18: Chamber pressure of several pulses (overlaid) of a 30-pulse train. I-bits for the corresponding pulses are shown in the graph inset.

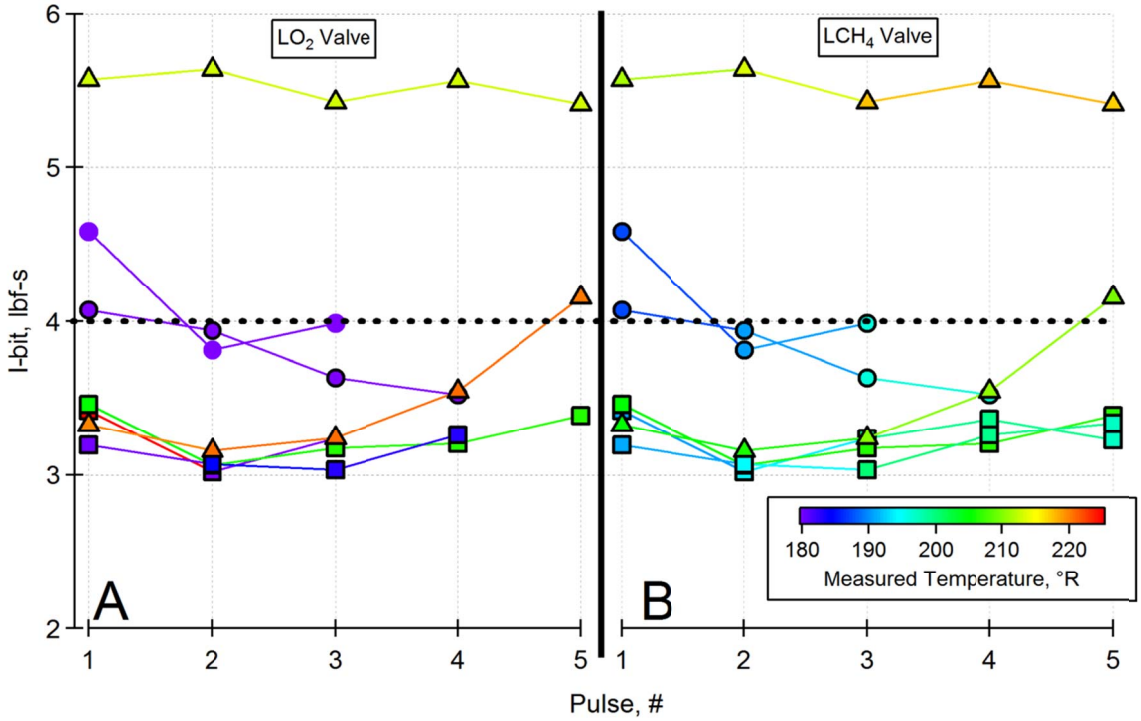

Figure 19: I-bit for each 40-ms EPW pulse with (A) LO_2 and (B) LCH_4 propellant inlet temperatures indicated by color. The dotted line indicates the minimum impulse bit (MIB) target of 4 lb_f-s.

6.3 Compact Unison Exciter

During the pulse test series, the engine was also tested with the compact exciter unit developed by Unison. The igniter proved reliable and capable of successfully igniting the engine through 80- and 40-ms EPW, at a 5-percent duty cycle for a train of 30 pulses (at 80-ms EPW). Performance was similar to other igniters and was not expected to change I-bit performance, thus the Unison data was not distinguished from the other test data. The only aborts observed during testing with the Unison compact exciter (80-ms EPW) were delayed ignition events described in Section 4.7.1 above. During testing of the 40-ms EPW, non-ignition events occurred, but given the length of an ignition delay (see Section 4.7.1), it is possible these were late ignition events that fell outside the EPW window, given how reliably the exciter operated otherwise. Figure 5 is a photograph of the engine operating with the compact Unison exciter.

6.4 Anomalies Observed During Test Series

Throughout the test series, several anomalies were observed that either affected the quality of results or which were notable, unexpected events. They are discussed here for completeness, and include thrust stand ringing, thrust stand zero drift, double pulsing, feed system temperature rise, and damage to the nozzle columbium coating.

6.4.1 Thrust Stand Ringing

As mentioned in the uncertainty analysis, Section 6.1, significant oscillations were observed in the thrust signal during pulses. This oscillation was not observed in chamber pressure traces (P_{cav}) or the feed system, suggesting the oscillation was caused by the natural frequency of the thrust stand itself. Figure 20 illustrates thrust stand oscillations during pulses from a single run (Run 243). A fast Fourier transform (FFT) of the data indicated these occurred at approximately 45 and 100 Hz. In $I_{sp,vac}$ performance data (Run 099) from prior testing (Ref. 7), similar oscillations were noticed during the startup transient. These dampened significantly towards the latter half of a 5-s burn, with the shutdown transient showing only the smaller 45 Hz oscillation. Since the oscillations dampen during the burn, they are likely due to natural frequencies of the thrust stand and the impulsive nature of startup transients. To date, no impact hammer-type test was conducted on the thrust stand to determine the natural ring-out frequency of the test stand. In addition, this behavior was also seen in prior pulse testing by Aerojet (Ref. 5), who presented a plot of the oscillating thrust, albeit for a different serial number injector. A rough estimation of this frequency

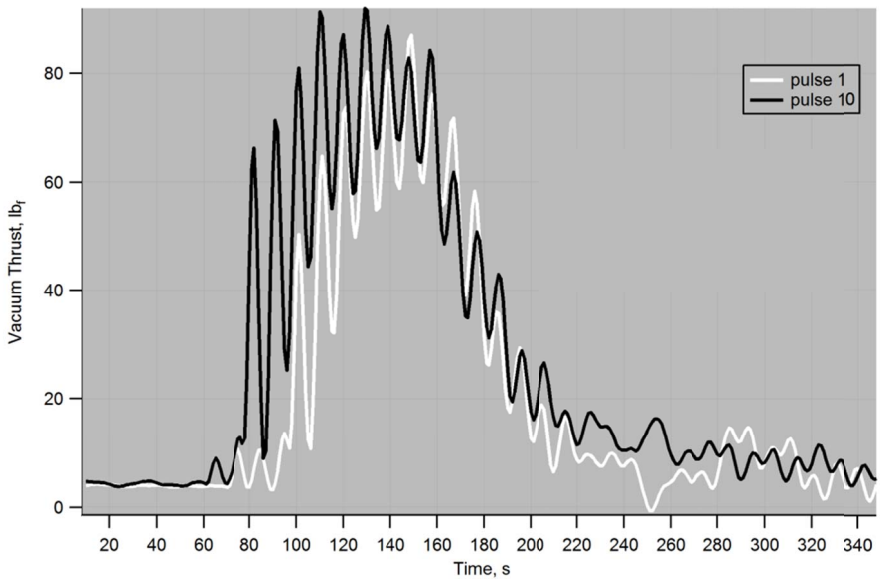

Figure 20: Thrust stand ringing for two representative pulses.

suggests a 100-Hz component. An FFT of some unpublished Aerojet data (Ref. 17) for this specific injector serial number indicated a 50-Hz oscillation, during a pulse test under similar conditions to the pulse run discussed in Figure 20 (Run 243). Since Aerojet did not make any indication (Ref. 5) of efforts to filter pulse data for thrust stand ringing, it was decided to present the current data for direct comparison, noting the oscillation similarities between data sets.

6.4.2 Thrust Stand Zero Drift

Over the course of longer (>20) pulse trains, the zero offset for the thrust levels shifted down by approximately 4 to 6 lb_f (17.8 to 26.7 N) (Figure 21). The cause for this is attributed to thermal expansion effects. The injector assembly is held in place by a threaded coupler, which reduces some of the cantilever loads, as seen in Figure 22. During testing, the engine mounting bracket experienced significant thermal loads due to the chill-in of the engine. These loads could have translated to the threaded coupler, which contracted, thus pulling on the engine assembly. This would have changed the force distribution on the load cells, resulting in the zero offset drift. As the assembly warmed up between tests, this load would relax, returning the engine to the original zero. I-bit calculations were adjusted to account for this effect (thrust values were rezeroed between each pulse). The drift altered I-bit results by ≤0.5 lb_f-s (2.2 N-s), but the overall trends are maintained (Figure 23).

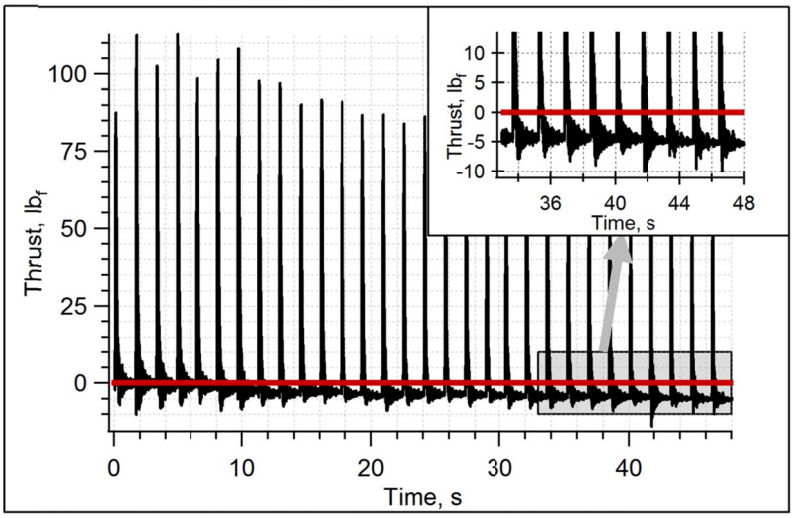

Figure 21: Thrust measurements over a 30-pulse train, illustrating thrust zero drift towards end of train (inset).

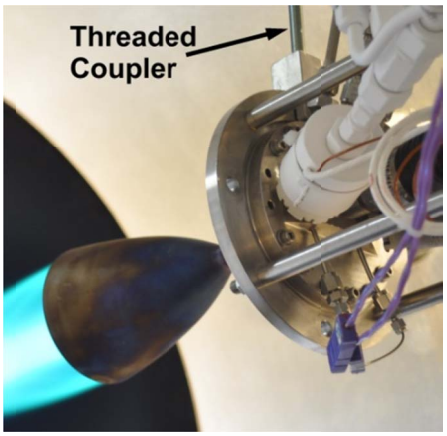

Figure 22: Photograph of engine showing threaded coupler (indicated) used to reduce cantilever loads.

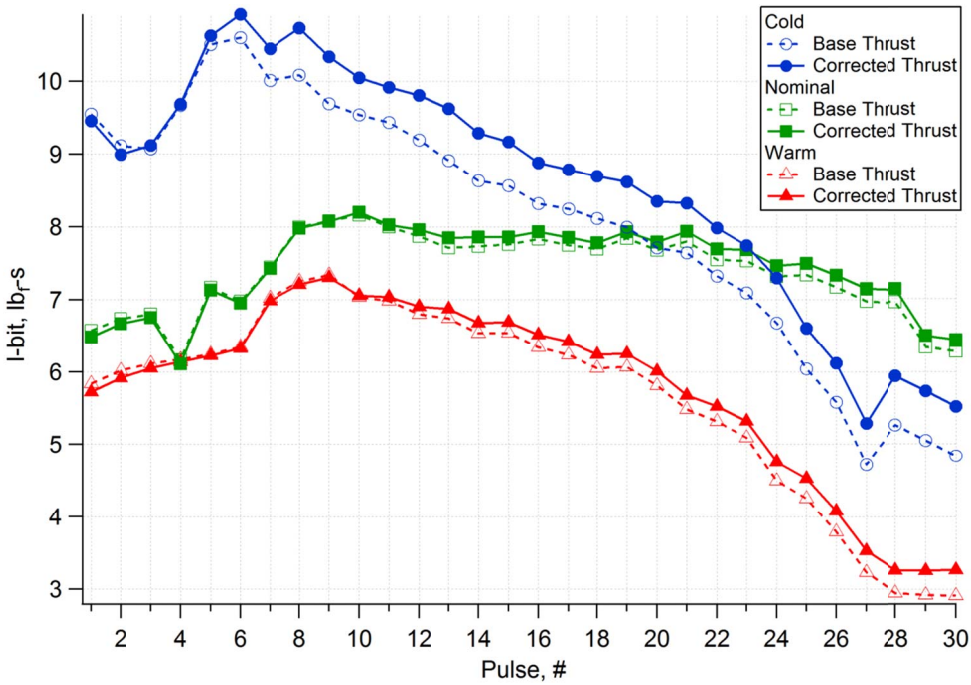

Figure 23: Effect of thrust zero drift on individual pulse I-bit results.

6.4.3 Double Pulse Phenomenon

A unique phenomenon was observed whereby the pulse regained strength after the valves had closed, as indicated visibly by a second flame pulse. This double pulse is best described using Figure 24, which shows a sequence of video images from a burn. The nominal, main pulse is shown in images 1 to 6, but in image 7 the flame regains strength. While the duration of the secondary pulse varies, this figure is representative of the behavior. Secondary pulses are not fully expanded and have a more disperse flame. Because the video frame rate is only 30 Hz, the visualization of the phenomena could not be directly correlated with the 1000-Hz data.

The effect on performance can be seen in Figure 25, where the chamber pressure traces for several pulses in a test at nominal propellant temperatures are overlaid. The inset shows the corresponding I-bits for all the pulses. The I-bits are highest during the double pulses. The reason is evident in the chamber pressure plot, where the dotted line at 17.5 psia (0.12 MPa) indicates the end of the I-bit integration time. The pressure decay is slower when a double pulse occurs, leading to a longer integration time and thus a higher I-bit. However, the chamber pressure data fails to reveal any feature that definitively indicates when the second pulse begins or ends. For example, the inflection point at around 0.15 s may be an indicator, but this also occurs for pulse 29, when no double pulse was observed.

One possible cause of the double pulse is suggested in Figure 26. The propellant temperatures in the manifold for both fuel and oxidizer are shown in Figure 26(A). The methane temperature behavior remains consistent throughout the test, but at 12 s (pulse 8), the oxygen temperature plummets, crossing over to a saturated state in the highlighted region of the graph. Figure 26(B) shows the corresponding oxygen manifold pressure. When there is liquid in the manifold, the pressure fails to return to its zero value between pulses. This could be a result of LO_2 vaporizing in the manifold after the oxygen valve has closed. Since the methane valve closes 40 ms after the oxygen, both reactants are present in the chamber. Thus, a flame could continue, or reignite, after the oxygen valve was commanded closed. It should be noted that the double pulse region does not exactly correlate with the saturation region in Figure 26. This temperature is only a point measurement taken at the entrance to the manifold, and elsewhere in the manifold system the temperature may be such that propellant exists in a different state than indicated by the manifold instruments.

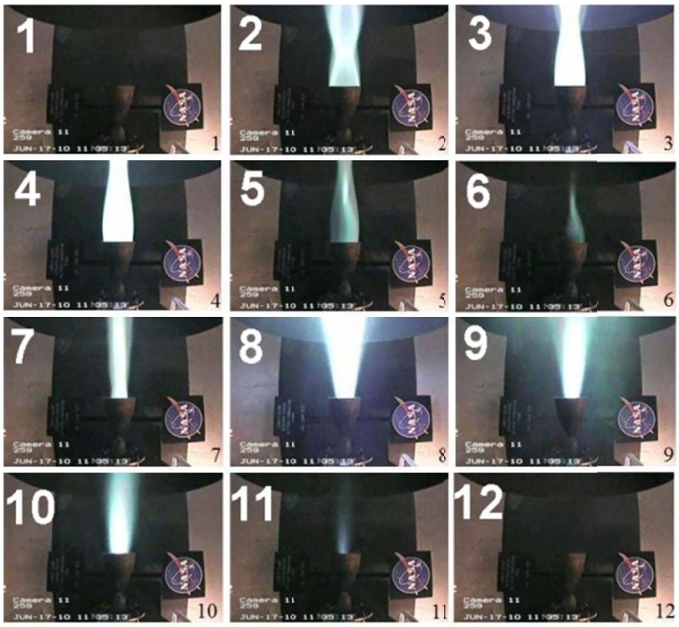

Figure 24: Image sequence illustrating the double pulse phenomena. The main pulse is shown in images 2 to 6, and the secondary double pulse begins in image 7.

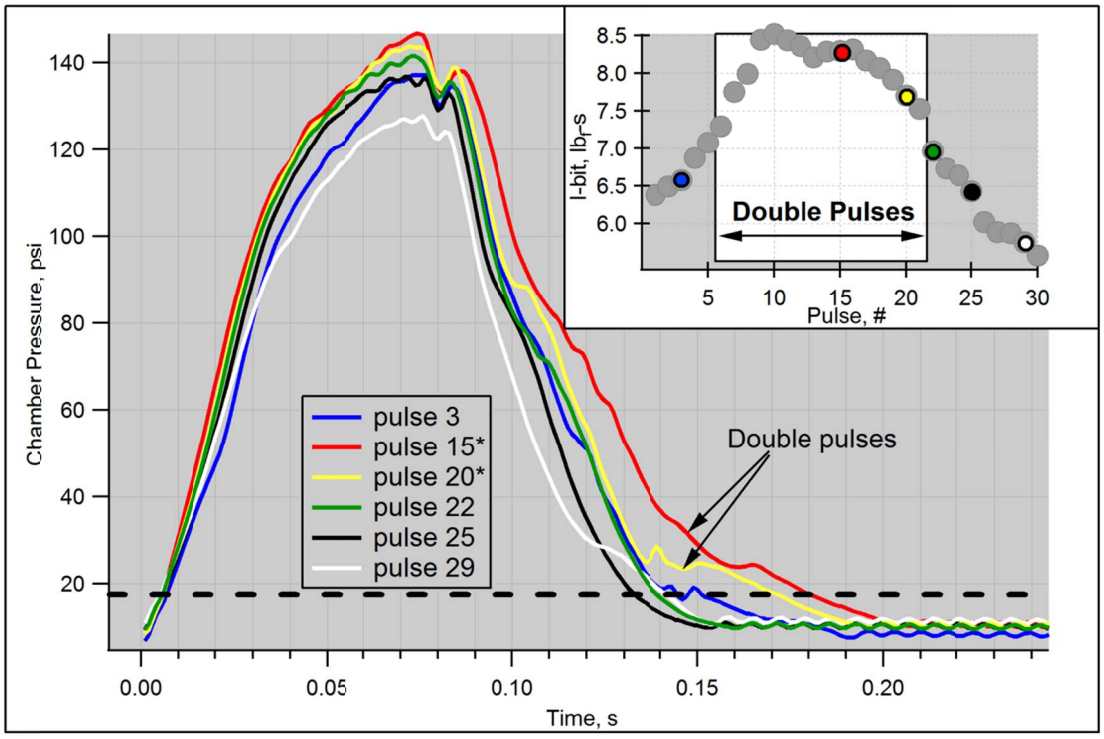

Figure 25: Chamber pressure of several pulses (overlaid) of a 30-pulse train with I-bits shown in the graph inset. The pressure decay for the double pulses (pulses 15 and 20) is slower, leading to a longer integration time for I-bit.

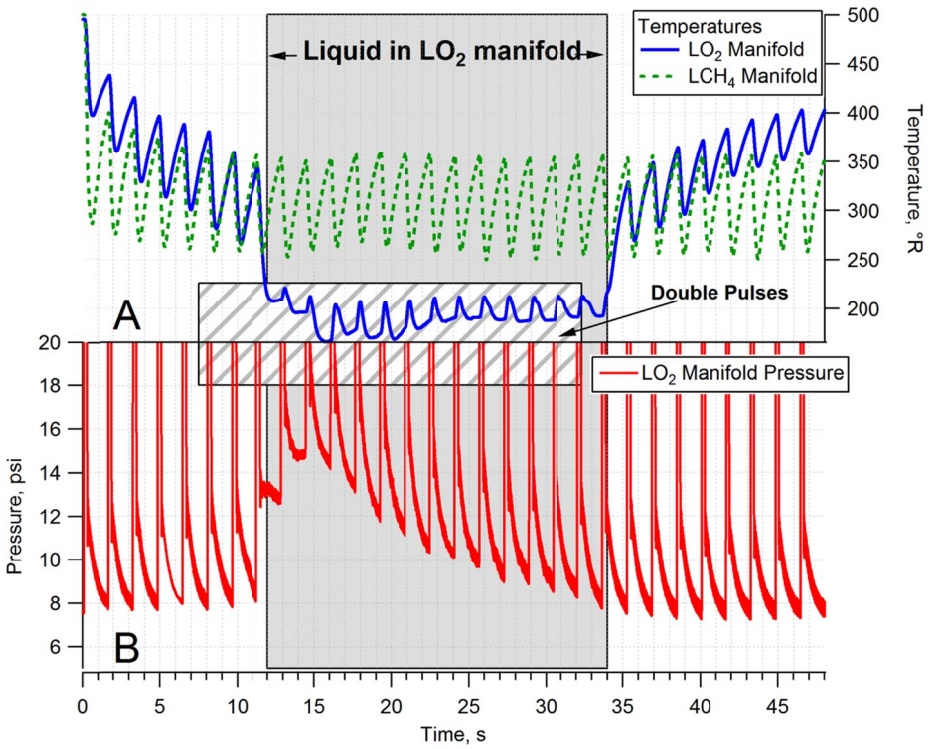

Figure 26: Saturation in the LO_2 manifold is indicated in the (A) manifold temperature and (B) LO_2 manifold pressure. Double pulses (box) overlap this saturation region.

Figure 27 illustrates the effect of the propellant temperature conditions on this phenomenon as indicated in the title of each plot. The oxygen manifold temperature is shown for all nine 30-pulse train tests. The highlighted region is where double pulsing was observed. The darker colored portions of the temperature traces indicate saturation (calculated using the manifold pressure at each point). The double pulse phenomenon is most prominent in the cold and nominal tests, where the majority of the 30 pulses showed double pulsing. This is supported by the temperature traces that indicate that the oxygen is liquid in the manifold for much of these tests. There is fluctuation between liquid and gas for several tests, such as Run 285, which may suggest a two-phase, or borderline condition. In contrast, double pulses are infrequent during tests at warm propellant conditions. While the data suggests the liquid is in a saturated state in the manifold, the temperature shifts are more severe, perhaps indicating that the propellant is experiencing different bulk conditions than the localized thermocouple indicates.

Another feature was observed in conjunction with the double pulsing; the pulses began to grow weaker after the double pulsing had subsided. Visually, these appeared to be shorter lived than pulses early in the train (prior to the double pulsing). This phenomenon was most noted during the warm propellant tests and could be quantified in two ways using the video: first, by the number of frames which displayed a visible flame, and second, by the intensity of the flame while present. Counting the number of video frames for each pulse revealed that most standard pulses lasted approximately four frames while weak pulses lasted two to three frames. However, the video frame rate was 30 Hz (33 ms/frame) and the propellant flow was active for 80 ms. Therefore, given the temporal resolution of the video, the difference between normal and weak pulses is not clear by frame count alone.

The intensity of the flame was quantified by measuring the luminosity in each frame of video. The image was converted to 8-bit gray scale. A line profile tool (Ref. 18) was positioned 10 pixels downstream of the nozzle exit, and the mean luminosity across the line was determined. This was done in each video frame of the main pulse flame, and the values were summed. For double pulses, separate measurements were done for the secondary flame. Figure 28 (right axis) shows the main pulse luminosities from Run 265 at warm propellant conditions. In this test, the luminosity seems to have a

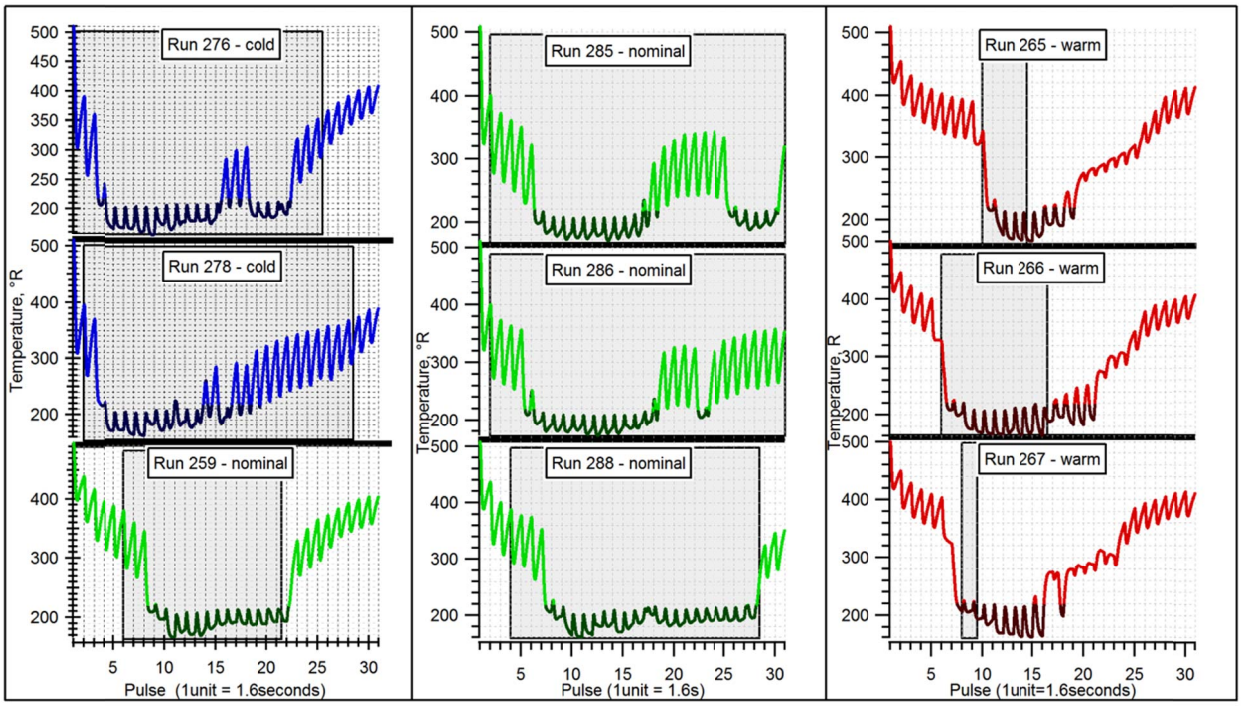

Figure 27: LO_2 manifold temperatures are plotted for each 30-pulse train run. Double pulses were observed in the highlighted areas, and the darker color of the trace indicates the temperature is below the saturation condition.

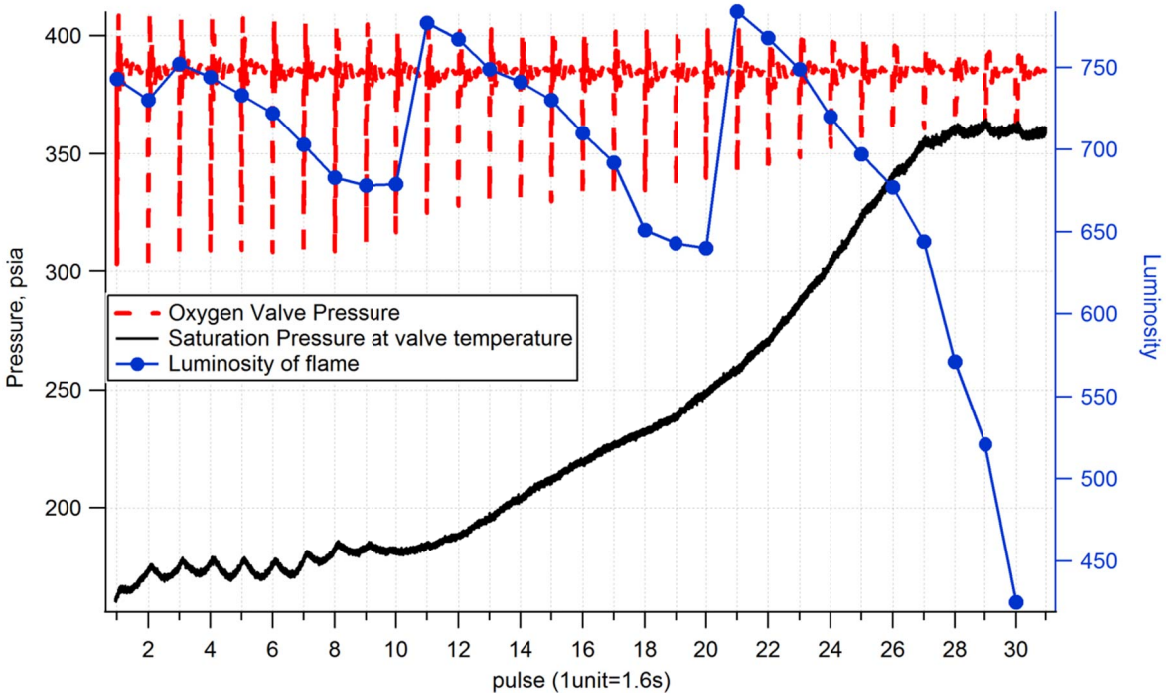

Figure 28: The summed luminosity from each pulse video frame indicates the weak pulse phenomena. The pressure traces indicate gas in the manifold at pulse 27. (Note that a measured luminosity of 100 is white saturation.)

cyclic feature, where the non-monotonic behavior at pulses 10 and 20 correspond to phase changes in the manifold (Figure 27). The last nine pulses show a weakening flame. The other traces on this plot represent the oxygen valve pressure and the corresponding saturation pressure (calculated using the measured valve temperatures). In the last four pulses, where the luminosity decrease is most notable, the valve pressure meets the saturation curve. This suggests transition to gas in the valve may be causing the weak pulses.

6.4.4 Temperature Rise in Feed System

Since the weak pulse phenomenon seems to be related to propellant warming, the question becomes the location of the heat source. As shown in Figure 29, the warming trend is not isolated to the oxygen valve. This warming trend is counterintuitive; one would expect the hardware to cool while cryogenic propellants are flowing through the system. (Note that the effect of this temperature rise on I-bit performance is represented in Figure 16.) Temperature measurements along the inlet lines are plotted in Figure 30 with the locations indicated in the schematic. The valve temperatures show some initial fluctuations before steadily rising. The two upstream locations, venturi and flow meter 1, show steady or shallow slopes during the valve instability, and then begin to rise with the valve temperature. However, the location between the two turbine flow meters is unique. The temperature is higher than any of the others, and the increase occurs here first. (The vertical lines indicate the slope rise of this flow meter temperature and valve temperature.) Thus, it appears that the heat rise initiates at this location. This may be due to recirculation or poor rotation of the turbine flow meter. During previous specific impulse testing (Refs. 6 and 7), observed pressure transients were also traced to this location. This flow meter was removed after the pulse testing, but subsequent tests for validation of this theory have not been done.

While engine heat soak back has not been definitively ruled out as a contributor, it is an unlikely factor in the temperature rise for two reasons. First, the flow meters are not in direct line of sight of the engine nozzle. If soak back was a factor, components in direct line of sight or connected to the engine, such as the valves, should see heat rise first as expected from radiative or conductive principles. Secondly, in the later pulses, the engine throat does not radiate as brightly suggesting the chamber is not experiencing as much heating from combustion (either from cooler flame or better wall cooling). Yet, there is no indication from the temperature plots that the heating of the lines has subsided.

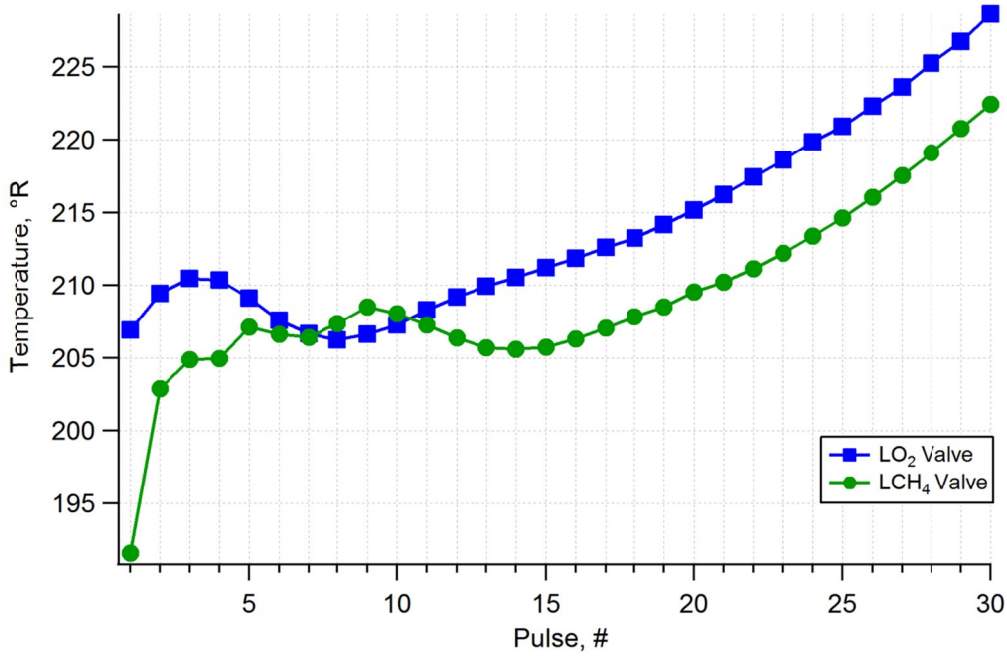

Figure 29: Propellant valve inlet temperatures for each pulse indicate a temperature rise during the pulse train.

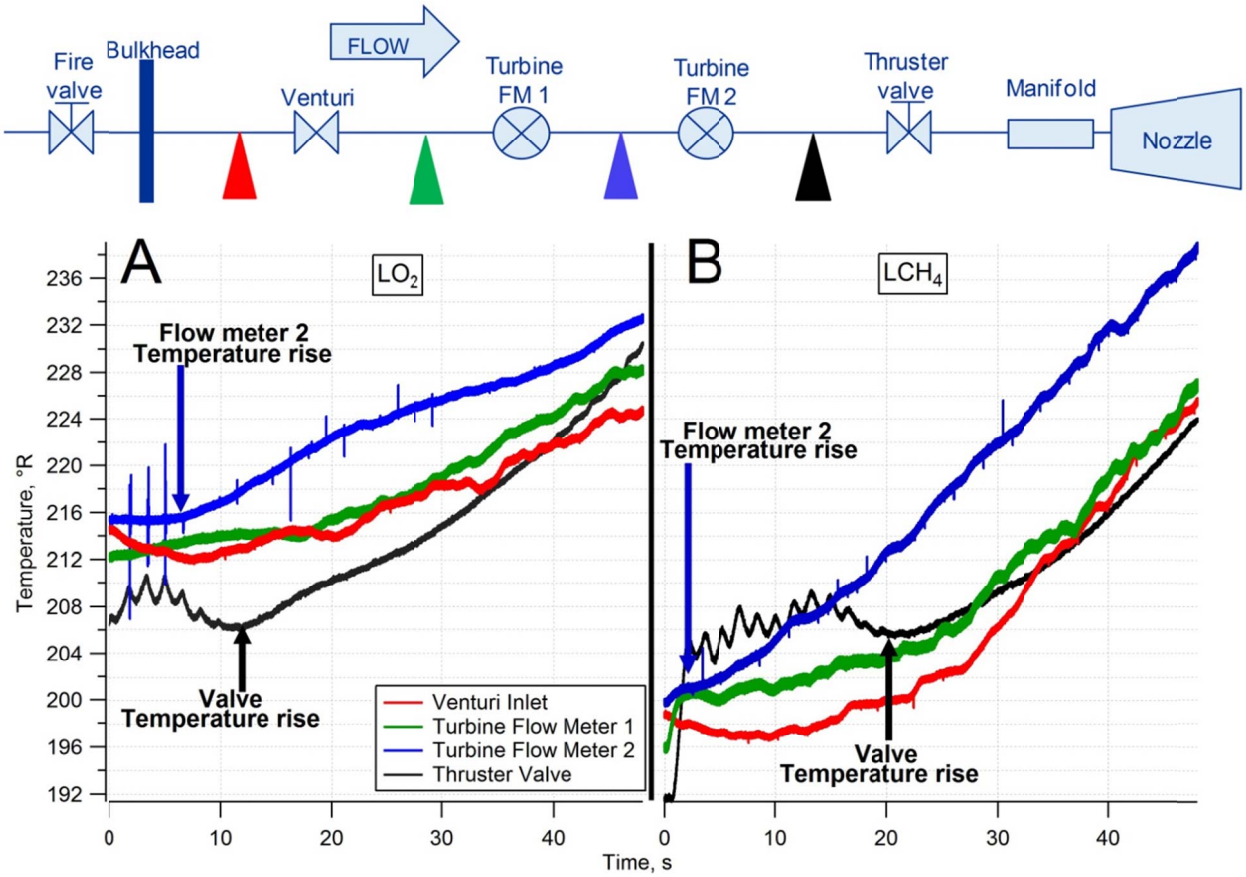

Figure 30: Feed system temperatures for (A) LO_2 and (B) LCH_4 lines. Corresponding sensor locations are shown in the above schematic.

Another source of potential warming in the propellant lines was the trace cooling and propellant bleed lines. These lines circulated liquid argon or liquid nitrogen around the propellant lines to thermally condition the propellant prior to a run. This cooling system was manually adjusted to meet such test needs that trace cooling may have been on or off for a given run. Using bleed valves in the propellant lines, a portion of the propellant could also be vented just upstream of the thruster valves as a means of maintaining propellant line temperature. These valves were closed for zone 2, and thus the non-flowing propellant during the dwell portions of zone 2 would be susceptible to line warming. Since the turbine flow meters were large masses relative to the rest of the propellant lines, it is likely that heating would begin in this vicinity. Additional insulation was installed following this test series as a further precaution against propellant warming.

6.4.5 Columbium Coating Damage

Two columbium nozzles were used during the course of this test program, both of which experienced some degree of damage to the inner chamber surface. The damage was revealed in routine visual inspections of the chamber, which occurred after every test day. The resulting boroscope images are shown in Figure 31 for both chambers. For nozzle SN–3 (Figure 31(A)), pitting and spalling of the surface coating was prevalent throughout the combustion chamber. In the second nozzle, SN–1 (Figure 31(B)), the pitting was isolated only to a few small spots. The coating is meant to prevent the oxidation of columbium (niobium), so a coating failure could ultimately lead to mechanical failure of the chamber if not addressed.

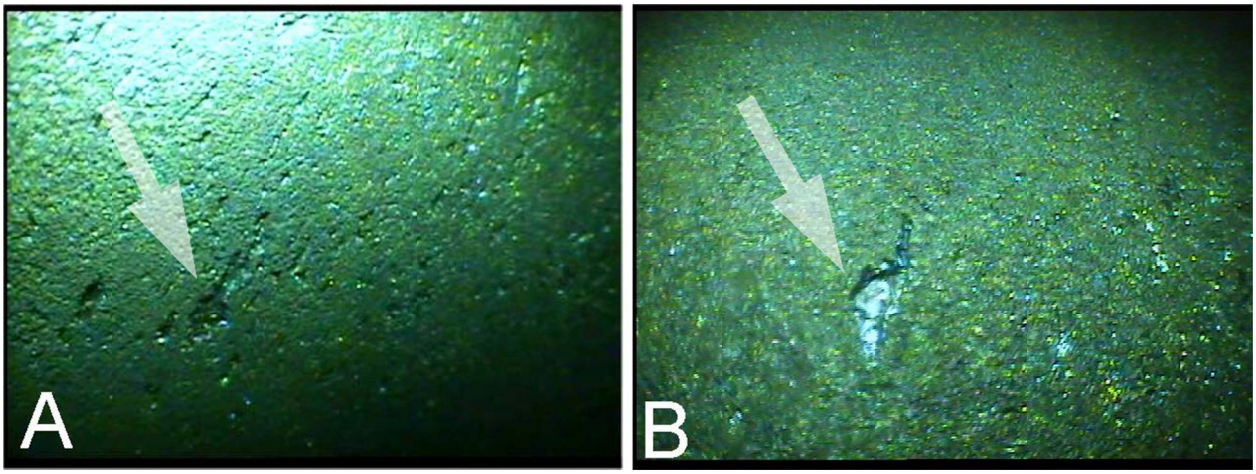

Figure 31: Coating damage on (A) SN–3 and (B) SN–1 chambers.

Figure 32: Sparks appearing in the plume during two tests with the SN–3 chamber are likely related to the coating damage.

The first chamber, SN–3, was damaged during the first pulse test day that used propellants at nominal temperature conditions. This test day consisted of 95 pulses at a 50-percent duty cycle totaling 38 s of burn time. (Prior to pulse testing the nozzle had undergone 131 s of specific impulse testing.) Since the chamber inspection can only be done at the end of the day, it is difficult to pinpoint which test caused the damage. However, sparks were observed in the final two tests, at the end of the 20-pulse trains (Figure 32).

The damaged SN–3 chamber was then replaced with a previously unused nozzle, the SN–1. A more benign test set was chosen: a 25-percent duty cycle with no more than five pulses per test and no more than seven tests per day. Minor damage was found on the third test day that used cold propellant temperatures. The chamber had undergone a total of 55 pulses with 5 s of accumulated burn time at all three propellant temperature conditions. Unlike the previous occurrence, there were no sparks or other indications in the plume. The nozzle itself had not yet been discolored by heat.

Even though the damage to SN–1 was minor, testing was halted until a cause could be identified. Table V summarizes some of the ideas that were explored after consulting with the engine manufacturer (Aerojet) and materials experts at Glenn (Ref. 19). Earlier testing of identical nozzles by Aerojet (both at the contractor's facility as well as NASA White Sands Test Facility (WSTF)) did not experience this damage, so many of these ideas relate to the differences in the test conditions.

The most probable cause of the damage, as suggested by the materials experts, is a chemical breakdown of the R512E silicate coating in a matter similar to "pesting." As the coating is exposed to heat and oxygen, a protective silica layer is formed, and volatilizes. If the oxygen or temperature

TABLE V: POTENTIAL CAUSES OF DAMAGE TO COLUMBIUM CHAMBER

Potential cause	Proof	Result
Nozzles used here were newer than ones used in previous testing. The coating batch on the new nozzles could have been flawed.	Test the old nozzle in the current facility in an attempt to cause the same damage.	Nozzle had been damaged by other means in previous testing and could not be reused.
Operating temperature exceeds the rated coating temperature.	No direct chamber temperature diagnostics are available; however, the color of the nozzle during burn is an indicator.	Nozzles discolor after heat exposure, but SN–1 had not yet been discolored. Yet the damage still occurred. Also, during duration testing, much higher temperatures were reached with no damage.
Molten material from a degrading of the spark plug damaged the nozzle.	Spark plug was removed and investigated.	No damage to the spark plug was found. No damage was observed in the igniter cavity nor at the converging section of the nozzle.
High local mixture ratios (*MR*s) near the wall were creating hot spots.	Igniter pins inspected for alignment. Rough calculations were done to determine local *MR* at the injector.	Pins are inspected as standard leak check procedures and were never found out of alignment. Calculations indicated a lower *MR* at the injector.
Propellant flow timing could be causing hard starts or oxidation on the walls (if directly exposed to LO_2).	Timing was reviewed. The oxygen valve was shut first so that the hot walls would not be exposed directly to oxygen.	Aerojet testing used a variety of timing conditions including oxygen flow on shutdown.

environment is insufficient, the rate of volatilization will exceed the formation, and the protective layer will fail. The oxygen may then leach into the coating and cause internal damage (scale formation). Small samples of the damaged coating were scraped off the chamber and chemically analyzed (x ray and scanning electron microscope (SEM)). The results (see Appendix B) indicated the presence of niobium oxide indicating oxidation of the substrate, but lacked the silica that would be indicative of the protective coating. The timing of the propellants had been oriented to avoid concern over too much oxygen near the hot walls, but this may have caused oxygen starvation of the coating. This, combined with the transient thermal conditions of a high duty cycle, could have led to break down of the coating. However, destructive testing and a more detailed materials study would be required to confirm this theory.

Various solutions were discussed including preconditioning of the nozzles in an oxide atmosphere or application of a barrier coating. However, the path forward involved a simple change in test conditions in an attempt to avoid or reduce the occurrence of the pesting phenomenon. After weighing the risks, testing was resumed with the SN–1 chamber (since damage was minimal) with the following changes:

(1) The duty cycle was decreased to 5 percent. The majority of the previous Aerojet testing had been done at this condition. This would also help mitigate the transients in the chamber, allowing more time between pulses for gas dispersion.
(2) The lower duty cycle also allows more time for the coating and substrate to reach thermal equilibrium between pulses. A thermal mismatch between the coating and substrate may also have contributed to the damage.
(3) The existing damage to the nozzle was well documented. When it was reinstalled, the nozzle was rotated 90° to see if the damage was related to the injector pattern (i.e., flow irregularities).

Following the above changes, chamber SN–1 was tested for over 700 pulses with videoscope inspections performed at the end of each test day. No further degradation of the coating was observed beyond expected normal wear. Since the nature of anomaly is beyond the scope of the testing program, and since no further damage was observed, it was concluded not to pursue a more definitive explanation of cause at this time.

7.0 Summary and Conclusions

The 100-lb_f liquid oxygen-liquid methane (LO_2-LCH_4) reaction control engine (RCE) developed by Aerojet was tested to determine impulse bit (I-bit) performance. All experiments took place in a reduced pressure environment using the Altitude Combustion Stand at the NASA Glenn Research Center. Propellant temperature was varied between three set point conditions to simulate operation limits of an in-space system. Pulse train length (number of consecutive pulses), pulse duration (electronic pulse width (EPW)), and duty cycle were all adjusted to meet test needs.

The performance fully met three of the four objectives set forth: It was operated at, and below, the required minimum pulse duration of 80 ms; it achieved a minimum impulse bit (MIB) of less than 4 lb_f-s (at 40-ms pulse duration); and it was operated at a range of duty cycle conditions. The fourth requirement stated that the MIB repeatability should be within ±5 percent after achieving stable temperature. However, stable temperatures were not achieved due to warming in the lines, believed to be associated with one of the turbine flow meters, though this has yet to be confirmed. This was a facility issue and not related to the performance of the engine. As a result, propellant temperatures increased gradually over the pulse train, which involved as many as 30 consecutive pulses. The I-bit values were shown to be strongly dependent on propellant inlet temperature with warmer propellants showing shorter I-bits. Thus the I-bit values dropped off toward the end of longer pulse trains. The number of consecutive pulses demonstrates reliable and repeatable ignition and pulse performance, bolstering the feasibility of this propellant combination for future exploration endeavors.

Several issues with this particular engine system did occur. A unique phenomenon was observed whereby the engine reignited immediately after the valves were closed, resulting in a “double pulse.” Manifold temperature and pressure conditions indicate that this may have been due to a two-phase flow condition. Vaporization of liquid in the oxygen manifold could have reacted with the lagging methane flow to cause a short re-ignition. This double pulse phenomenon also led to higher I-bits (due to longer integration times). Another issue was damage to the chamber surface coating that occurred early in the pulse test program. Since the coating prevents oxidation of the columbium substrate, this posed a concern to the safety of the engine. Chemical analysis of some damaged coating material indicates this may have been caused by a phenomena likened to pesting. Insufficient oxygen at these temperature conditions prevented the formation of silicon oxide on the coating surface. The lack this protective layer caused internal damage to the coating (scaling). The thermal cycling of a high duty cycle could have contributed to this issue. Testing was resumed at lower duty cycle conditions (5 percent) with no further damage.

8.0 Related Work

Testing with this engine continued with a focus on ignition phenomena. Since one of the perceived drawbacks of this propellant combination is high ignition energy, this program sought to determine energy limits. A well instrumented exciter unit was used to obtain high-fidelity voltage information of the spark discharge. By coupling this to the existing pressure instruments, it was possible to determine the energy of the ignition spark. A variable energy exciter unit was developed to explore these limits.

References

1. Melcher, J.C. and Allred, J.K., "Liquid Oxygen/Liquid Methane Testing of the RS-18 at NASA White Sands Test Facility", AIAA 2008-4843, *44th AIAA/ASME/SAE/ASEE Joint Propulsion Conference and Exhibit,* Hartford, CT, July 21–23, 2008.
2. Melcher, J.C. and Allred, J.K., "Liquid Oxygen/Liquid Methane Test Results of the RS-18 Lunar Ascent Engine at Simulated Altitude Conditions at NASA White Sands Test Facility," AIAA 2009–4949, *45th AIAA/ASME/SAE/ASEE Joint Propulsion Conference and Exhibit,* Denver, CO, Aug. 2–5, 2009.
3. Over, A.P., Klem, M.K., and Motil, S.M., "A Successful Infusion Process for Enabling Lunar Exploration Technologies," AIAA 2007–6196, *AIAA Space 2007 Conference and Exposition,* Long Beach, CA, Sept. 18–20, 2007.
4. Stone, R., Tiliakos, N., Balepin, V., Tsai, C.-Y., and Engers, R., "Altitude Testing of LOX-Methane Rocket Engines at ATK GASL," AIAA 2008–3701, *26th AIAA Aerodynamics Measurement Technology and Ground Testing Conference,* Seattle, WA, June 23–26, 2008.
5. Robinson, P.J., Veith, E.M., Hurlbert, E.A., Jimenez, R., and Smith, T.D., "100-lb_f LO2/LCH4 - Reaction Control Engine Technology Development for Future Space Vehicles", *59th International Astronautical Federation,* Glasgow, Scotland, United Kingdom, September 29–October 3, 2008.
6. Marshall, W.M. and Kleinhenz, J.E., "Hot-Fire Testing of 100 lb_f LOX/LCH_4 Reaction Control Engine at Altitude Conditions", *JANNAF 57th JPM/7th MSS/5th LPS/4th SPS Joint Subcommittee Meeting,* Colorado Springs, CO, May 3–7, 2010.
7. Marshall, W.M. and Kleinhenz, J.E., *Performance Analysis of Specific Impulse Tests of a 100-lbf (445-N) LO2/LCH4 Reaction Control Engine at Altitude Conditions*, NASA/TM—2011-217131, National Aeronautics and Space Administration, Cleveland, OH, 2011.
8. *The Historic Rocket Engine Test Facility*, Produced by: NASA GRC, Available from: http://retf.grc.nasa.gov/, Last Accessed 2011.
9. Smith, T.A., Pavli, A.J., and Kacynski, K.J., "Comparison of Theoretical and Experimental Thrust Performance of a 1030:1 Area Ratio Rocket Nozzle at a Chamber Pressure of 2413 kN/m^2 (350 psia)," AIAA–87–2069, *AIAA/SAE/ASME/ASEE 23rd Joint Propulsion Conference,* San Diego, CA, June 29– July 2, 1987.
10. Pavli, A.J., Kacynski, K.J., and Smith, T.A., *Experimental Thrust Performance of a High-Area-Ratio Rocket Nozzle*, NASA TP–2720, National Aeronautics and Space Administration, Cleveland, OH, 1987.
11. *DIAdem: Getting Started with DIAdem*, National Instruments, Austin, TX, 2009.
12. Grasl, S.J., Skaff, A.F., Nguyen, C., Schubert, J., and Arrington, L., "Liquid Methane/Liquid Oxygen Propellant Conditioning and Feed System (PCFS) Test Rigs—Preliminary Test Results," *JANNAF 57th JPM/7th MSS/5th LPS/4th SPS Joint Subcommittee Meeting,* Colorado Springs, CO, May 3-7, 2010.
13. Skaff, A., Grasl, S., Nguyen, C., Hockenberry, S., Schubert, J., Arrington, L., and Vasek, T., "Liquid Methane/Liquid Oxygen Propellant Conditioning Feed System (PCFS) Test Rigs," *JANNAF 3rd Spacecraft Propulsion System Joint Subcommittee Meeting,* Orlando, FL, December 8-12, 2008.
14. Stiegemeier, B.R. and Marshall, W.M., "Sea-Level Testing of a 100 lb_f LOX/Methane Reaction Control Engine", *JANNAF 57th JPM/7th MSS/5th LPS/4th SPS Joint Subcommittee Meeting,* Colorado Springs, CO, May 3–7, 2010.
15. Lemmon, E.W., Huber, M.L., and Mclinden, M.O., *NIST Standard Reference Database 23: Reference Fluid Thermodynamic and Transport Properties-REFPROP, Version 8.0*, National Institute of Standards and Technology, Standard Reference Data Program, Gaithersburg, MD, 2007.

16. *JANNAF Rocket Engine Performance Test Data Aquisition and Interpretation Manual*, CPIA Publication 245, Chemical Propulsion Information Agency, Silver Spring, MD, 1975.
17. Aerojet, Telecon, January 20, 2010.
18. Klimek, R.B. and Wright, T.W., *Spotlight-16 Image Analysis Software*, Software Manual Version 2004.4.27, 2004.
19. Aerojet, Telecon, April 28, 2010.

Appendix A.—Acronyms and Symbols

The acronyms and symbols found in this report are presented here.

Acronyms

ACS	Altitude Combustion Stand
EPW	electronic pulse width
ETDP	Exploration and Technology Development Program
FFC	fuel film cooling
FFT	fast Fourier transform
JANNAF	Joint Army, Navy, NASA, Air Force
MIB	minimum impulse bit (lb_f-s (N-s))
MR	mixture ratio
NASA	National Aeronautics and Space Administration
NIST	National Institute of Standards and Technology
PCAD	Propulsion and Cryogenic Advanced Development (project)
PCFS	propellant conditioning feed system
PLC	programmable logic controller
RCE	reaction control engine
RETF	Rocket Engine Test Facility
RTD	resistance temperature detector
SEM	scanning electron microscope
SN	serial number
TFV	Fuel temperature measured just upstream of thruster valves, °R (K)
TOV	Oxidizer temperature measured just upstream of thruster valves, °R (K)
WSTF	White Sands Test Facility

Symbols

A	area, $in.^2$ (mm^2)
B	bias error
b	uncertainty value
C_d	discharge coefficient
c^*	characteristic exhaust velocity, ft/s (m/s)
F	thrust force, lb_f (N)
I-bit	impulse bit (lb_f-s (N-s))
I_{sp}	specific impulse, s
L'	characteristic chamber length, in. (mm)
$\dot{m}$	mass flow rate, lb_m/s (kg/s)
MR	mixture ratio, oxidizer/fuel (O/F), lb_m/s oxidizer / lb_m/s fuel (kg/s oxidizer / kg/s fuel)
P	pressure, psia (MPa)
$\mathcal{P}$	precision uncertainty
T	time, s
Q	volumetric flow rate, gal/min (L/min)
t	factor from Student's *t*-distribution

Δ	differential
ρ	fluid density, lbm/ft^3 (kg/m^3)

Subscripts

amb	ambient
c	chamber
calc	calculated uncertainty
cali	calibration uncertainty
cav	chamber acoustic cavity
e	nozzle exit
F	thrust force
f	fuel
ign	igniter
inst	instrument uncertainty
meas	measurement uncertainty
o	oxidizer
therm	thermal expansion effects
throat	throat
total	total
vac	vacuum condition

Appendix B.—X ray and Scanning Electron Microscope Results

Small samples of the coating from one of the damaged nozzles, serial number (SN)–3, were provided to the NASA Glenn materials group for analysis. The nozzle was scraped in both damaged and undamaged areas for comparison. Kapton® tape (DuPont) was used to collect and contain the sample. The following information is the raw data that led to the conclusions provided by Dongming Zhu of the NASA Glenn materials group, who performed this analysis.

X ray diffraction data was gathered using a D8 Advance Diffractometer using Cu Kα radiation. Data was also gathered on the D8 Discover Diffractometer (area detector) to check for grain size effects. Full even-intensity Debye rings were observed indicating good sampling statistics. Samples of light and dark Kapton tape were also run to determine the contribution of the tape to the background. The scan of the light tape corresponded well with both datasets.

B.1 X ray Diffraction: Undamaged (Baseline)

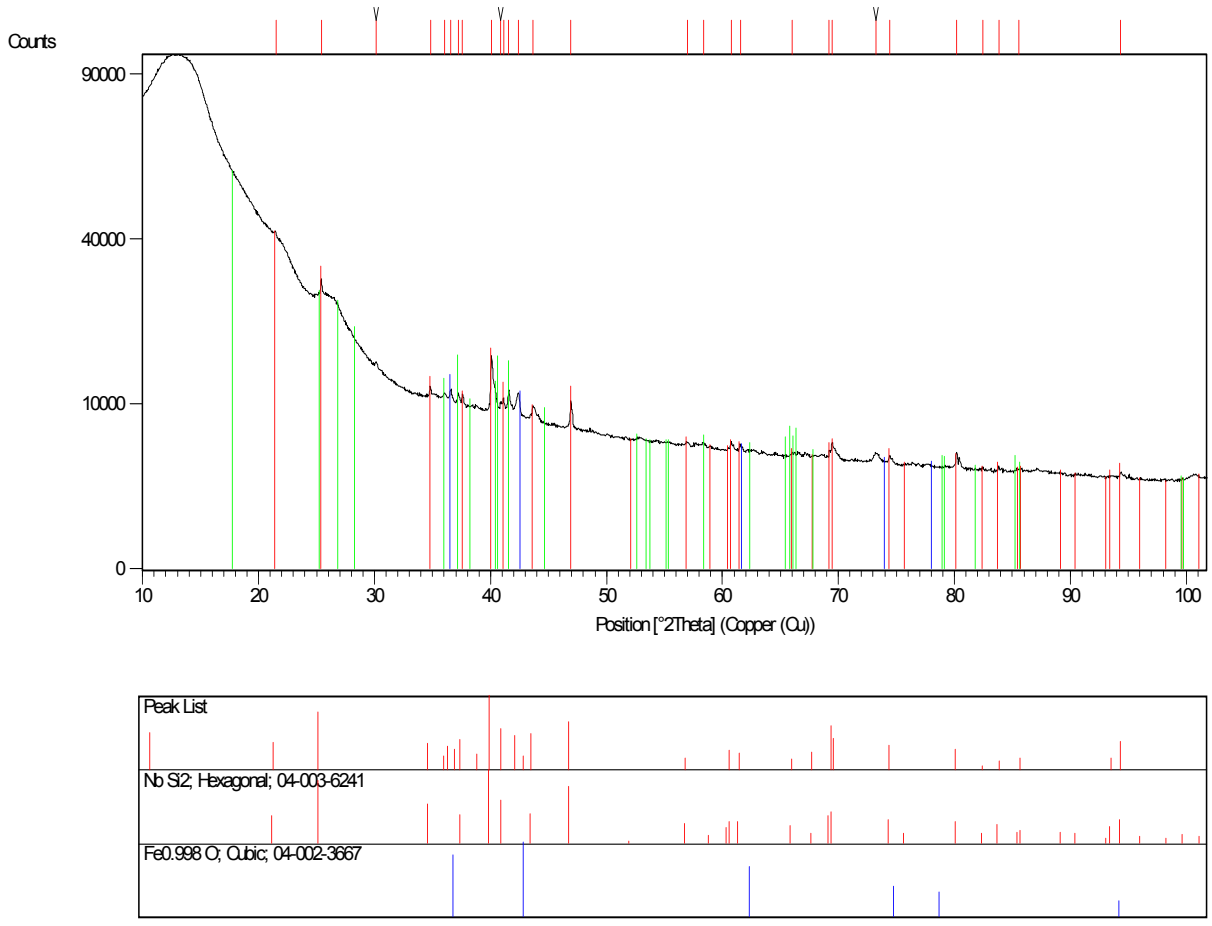

Phase ID sample:

Chemical formula	Compound name	Crystal system	Reference code	SemiQuant [%]
Nb Si2	Niobium silicon	Hexagonal	04–003–6241	93
Fe0.998 O	Wüstite, syn	Cubic	04–002–3667	7

Possible matches to single unidentified peaks (not shown in graphics):

30.1° Fe3O4, $Fe(Nb_2O_6)$, or Cr_2FeO_4
40.9° $NbCr_2$
73.2° FeO

B.2 X ray Diffraction: Damaged

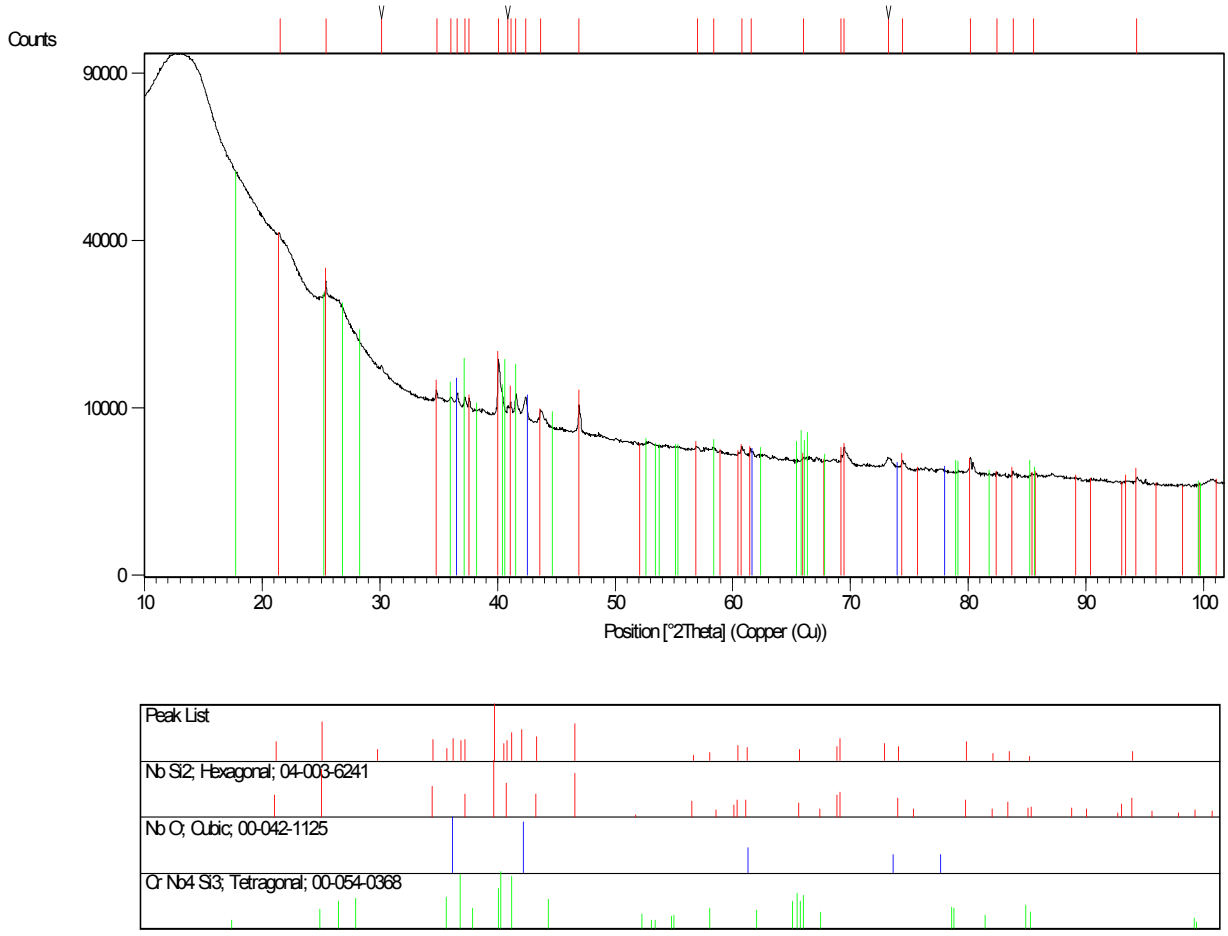

Phase identification sample:

Chemical formula	Compound name	Crystal system	Reference code	SemiQuant [%]
Nb Si_2	Niobium silicon	Hexagonal	04–003–6241	-----
Nb O	Niobium oxide	Cubic	00–042–1125	-----
Cr Nb_4 Si_3	Chromium niobium silicon	Tetragonal	00–054–0368	-----

Possible matches to single unidentified peaks (not shown in graphics):

10.9° a host of zeolite (SiO_2) phases
36.1° FeO (different lattice parameter than in table)
36.5° NbO
42.3° FeO (different lattice parameter than possible at 36.1° and table)
39.0° Fe_2O_3

B.3 Scanning Electron Microscope Undamaged

The black spots in the image indicate pore formation, which is limited. There is a high Nb peak, indicating the niobium substrate, and a high Si for the coating. The low O (oxygen) peak indicates that neither has oxidized.

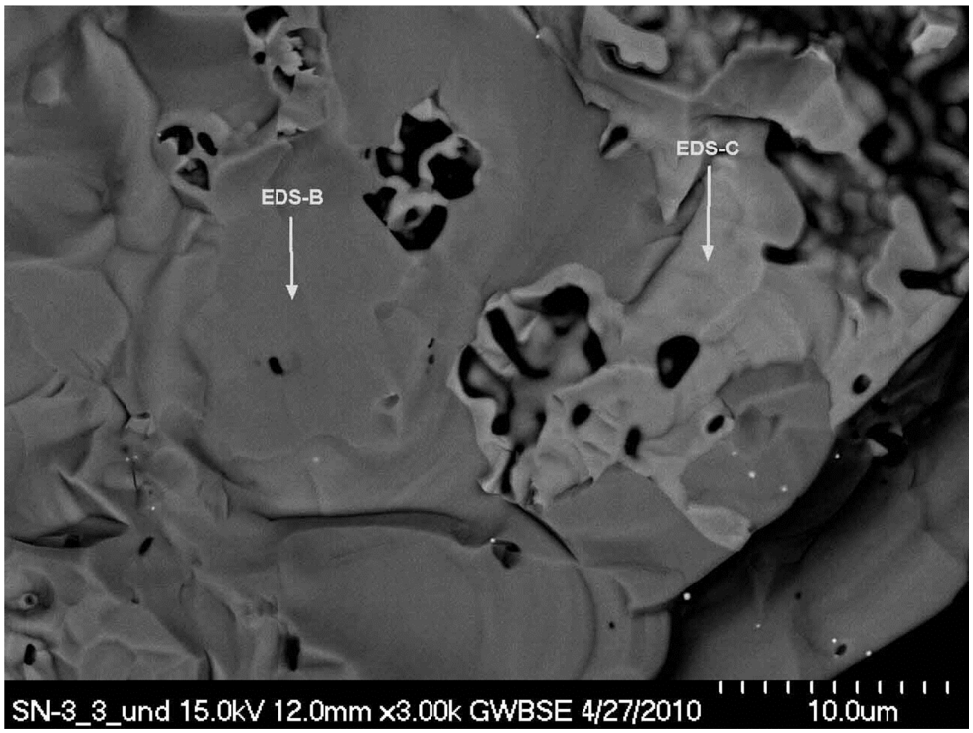

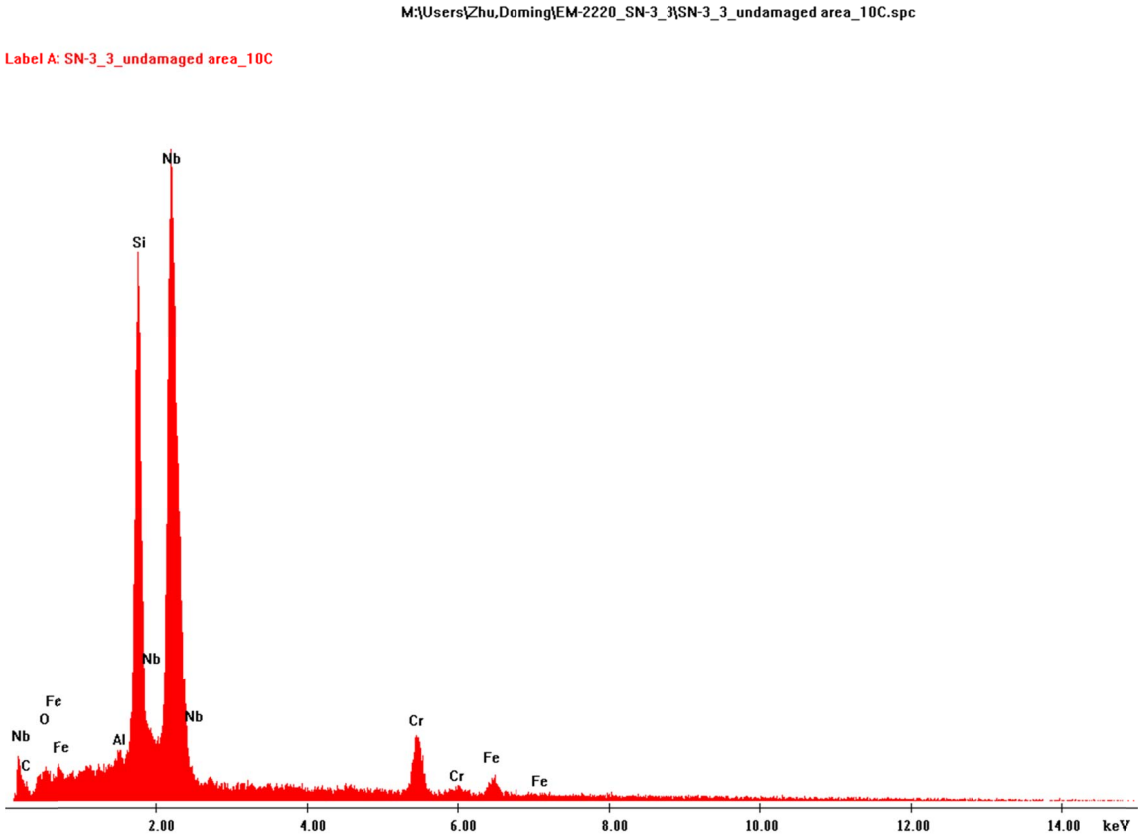
M:\Users\Zhu,Doming\EM-2220_SN-3_3\SN-3_3_undamaged area_10C.spc
Label A: SN-3_3_undamaged area_10C
Nb
Si
Nb
Fe
O
Nb
Fe
Al
Nb
C
Cr
Cr
Fe
Fe
2.00
4.00
6.00
8.00
10.00
12.00
14.00
keV

B.4 Scanning Electron Microscope Damaged

Area L shows the coating with very little protective oxidation. Areas J and K show evidence of substrate oxidation.

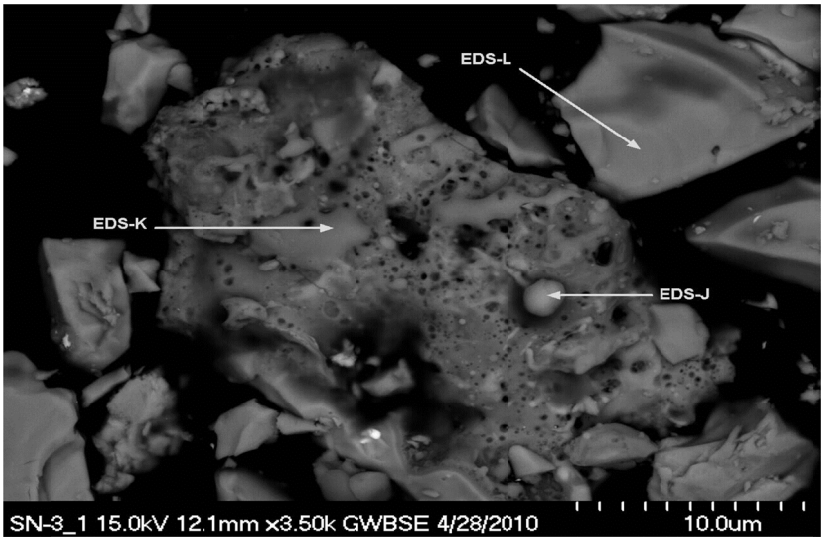

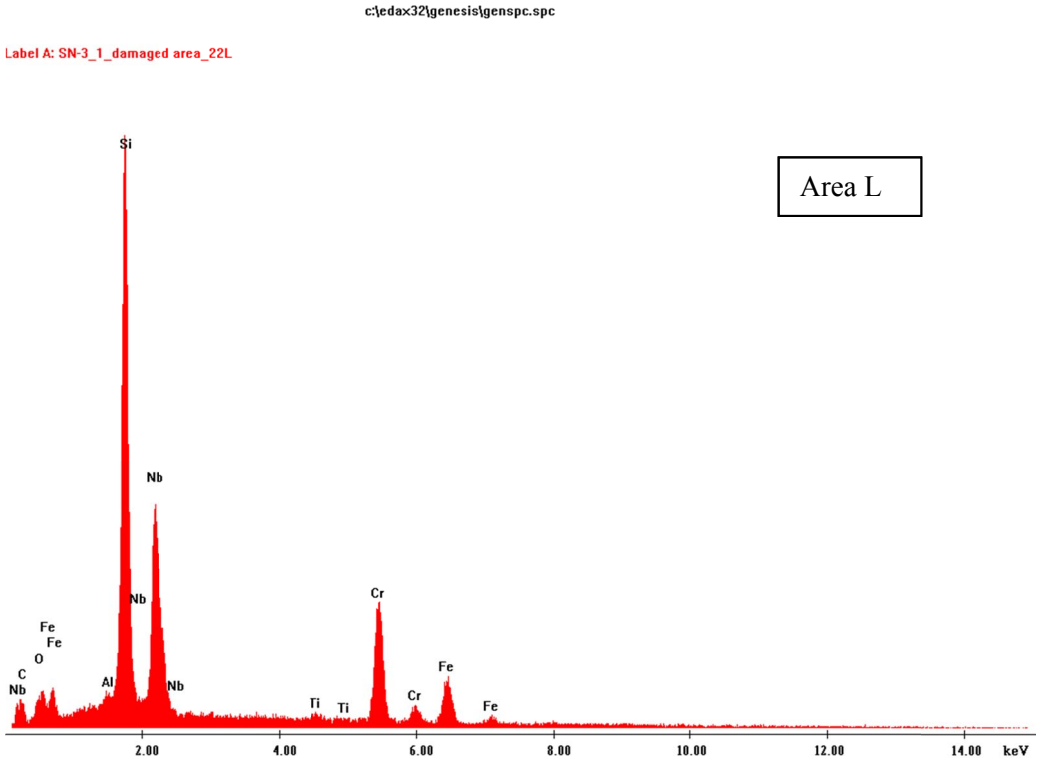

Area L

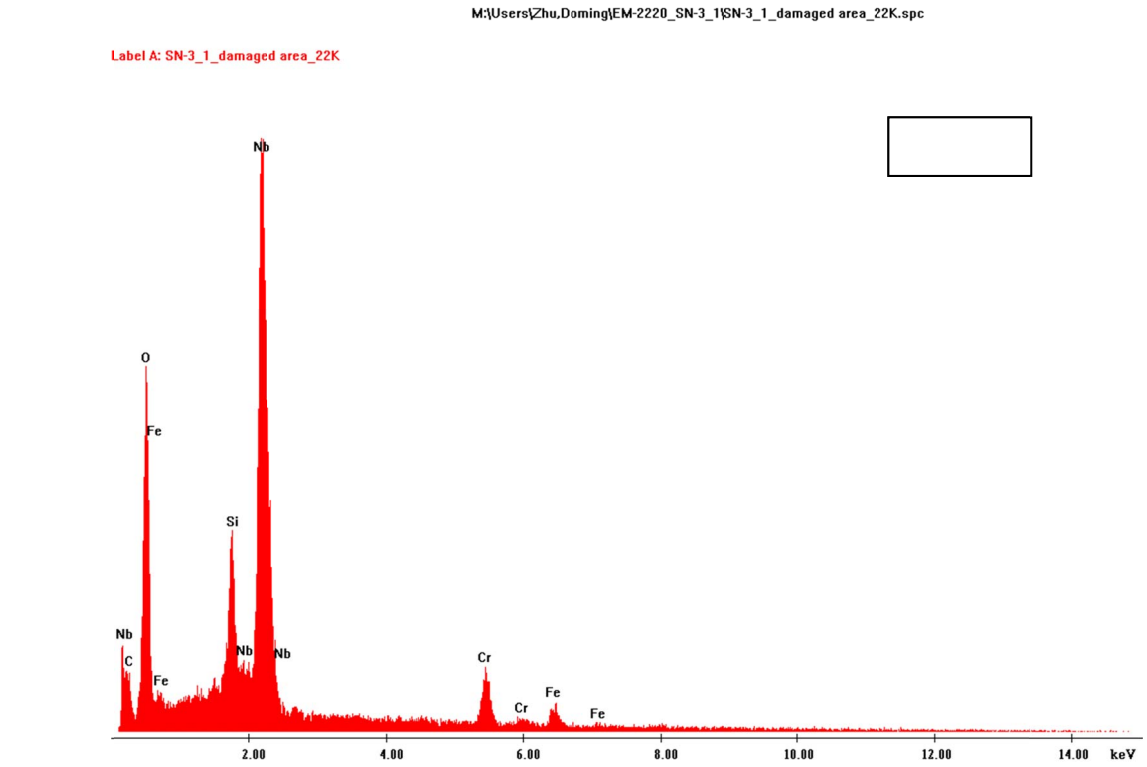
M:\Users\Zhu,Doming\EM-2220_SN-3_1\SN-3_1_damaged area_22K.spc
Label A: SN-3_1_damaged area_22K
Nb
O
Fe
Si
Nb
C
Fe
Nb
Nb
Cr
Cr
Fe
Fe
2.00
4.00
6.00
8.00
10.00
12.00
14.00
keV

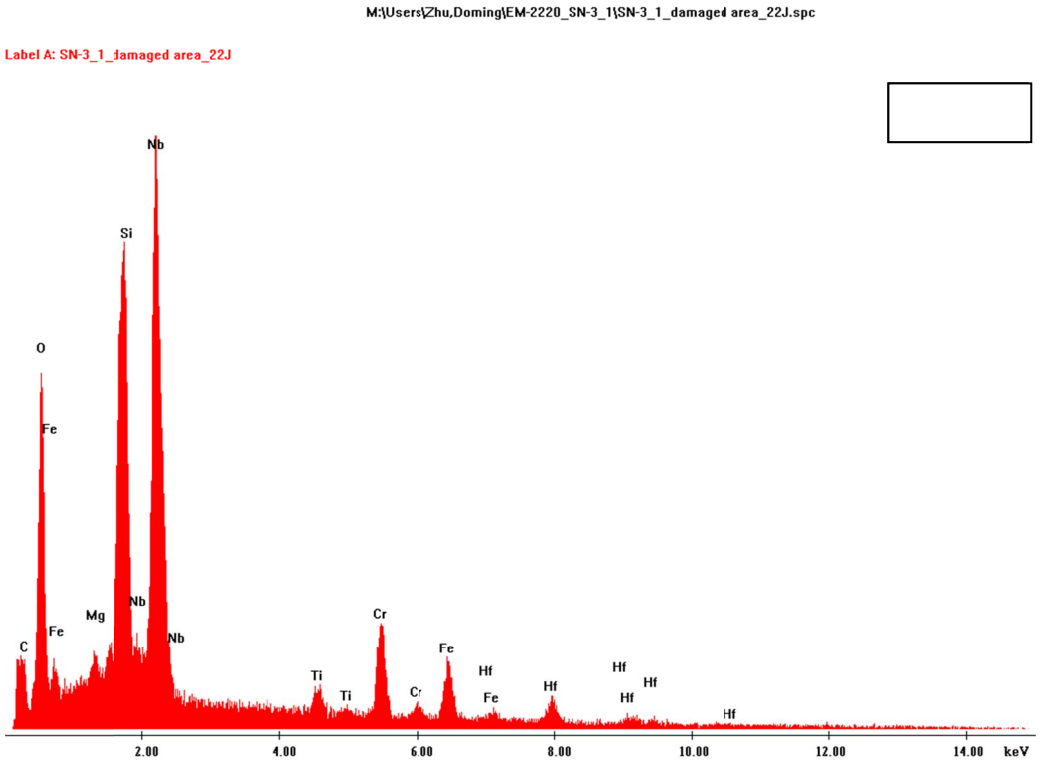
M:\Users\Zhu,Doming\EM-2220_SN-3_1\SN-3_1_damaged area_22J.spc
Label A: SN-3_1_damaged area_22J
Nb
Si
O
Fe
Mg
Nb
C
Fe
Nb
Ti
Ti
Cr
Cr
Fe
Hf
Fe
Hf
Hf
Hf
Hf
Hf
2.00
4.00
6.00
8.00
10.00
12.00
14.00
keV

Appendix C.—Test Data Log

The following tables list all tests that were performed as part of this study. The measurements are averages taken over the I-bit integration time. (Note that for high duty cycle (e.g., 50 percent) the chamber pressure never decays to 17.5 psi, which is the end point of the I-bit integration defined in Section 5.1. Therefore, the integration time ends when the next pulse begins). The information is abbreviated with respect to JANNAF standards to facilitate easier viewing of the parameters referenced in this document. The full table is available upon request.

Column descriptions:

(1) Run #: The number of the test run as referenced to the first facility tests in the 100-lb_f RCE test program.
(2) Test Description: The target conditions and/or purpose for the run is given.
(3) All successful hot fire tests are indicated by their target propellant temperature (nominal, warm, or cold).
(4) With the exception of a few tests, the flow rates were set to achieve a mixture ratio (*MR*) of 2.5 based on the previous specific impulse test series. There are a few conditions designated "MR Low" which used the set point for an *MR*=2.0.
(5) "Thrust Cal" indicates a calibration of the thrust load cell. All calibrations were performed at altitude conditions. These calibrations were performed at the beginning and end of each day
(6) "Late ignition" indicates that for one of the pulses in a given spark train, ignition occurred late. This triggered an abort, as described in section 4.7.1, which caused an incomplete (aborted) pulse train.
(7) "No-ignition" indicates that a given pulse in the train failed to ignite, resulting in an incomplete pulse train.
(8) "Abort" indicates a facility abort. This could be triggered by a sensor reading out of limit. In some cases, this was due to an overly conservative limit set in the PLC (e.g. for the manifold pressures POJ and/or PFJ).
(9) Pulse Duration: The time between ignition and the closing of the propellant valves for each pulse. This is also known as the electronic pulse width (EPW).
(10) Number of Pulses achieved/planned: The first number specifies the number of successful pulses achieved, while the second number indicates the number of pulses intended for the pulse train.
(11) Duty Cycle: This indicates the frequency of pulsing. It is the ratio of the pulse duration to the total between pulses (pulse start to pulse start). For example, a test with a 5-percent duty cycle and 80-ms pulse durations would mean there is 1600 ms between pulses (80 ms of hot fire and 1520 ms of down time).
(12) Run Tank Pressures: The pressure in the propellant holding tanks. This is a pressure-driven flow system, so these pressures govern the mass flow rate of the propellants, and thus the *MR*.
(13) Run Tank Temperature: The temperature of the propellant in the holding tanks. The desired conditions (cold, nominal, and warm) were judged based on the temperature at the thruster valves. Thus the run tank temperatures were chosen to account for line losses. Note the temperatures are given in Fahrenheit, since this was the convention of the propellant conditioning systems (PFCS).
(14) Thrust parameters: The thrust measurements from the load cell. The first column (Thrust, lb_f) is a summation of the three loads, corrected using the calibration coefficient or "K factor". The "vacuum thrust" is corrected to vacuum relative conditions.
(15) Mass Flow: The mass flow rates and corresponding mixture ratio, or *MR*, of the propellants calculated at the venturi. During these short pulse times, these measurements are highly transient (Section 4.4.1) and these numbers are rough averages.
(16) Chamber pressure: The pressure inside the combustion chamber, "P_{cav}" averaged.

(17) Valve temperature: The temperature at the propellant thruster valve. TOV is the oxidizer side, TFV is fuel.
(18) Test capsule pressure: The pressure in test cell. Therefore, the 'ambient' pressure of the engine.
(19) Average I-bit: The I-bits for each individual pulse are averaged to obtain this number.
(20) Note: Test specific notes.

RCE ACS Test summary: Pulse testing

Run #	Test description	Pulse Duration, s	Number of pulses achieved / planned	Duty Cycle	Run Tank Pressure, psig		Run Tank Temperature, Deg F		Thrust paramaters			Average Venturi Mass flow			Chamber pressure	Valve Temps (R)		Test Capsule pressure, psia	Average Ibit, lbf-s	NOTES
					LOX	CH4	LOX	CH4	Thrust (lbf)	Vac Thrust (lbf)	K Factor	LOX Venturi (lbm/s)	CH_4 Venturi (lbm/s)	MR venturi	Pcav (5607)	TOV (5511)	TFV (5011)			
Columbium Nozzle SN#3, Injector 6, Champion Exciter (contunation from steady state tests)																				
	Interim activity: Prepare for pulse testing, software modified.																			
3/5/2010	Day Plan: Begin pulse test program at nominal conditions. Start with 1s duration and low number of pulses, gradually decrease duration and incorperate more pulses. Target is to get 80ms duration.																			
	End of Day: Very sucessful day.**PCIGN broke at test 193**. Took time to work out facility timing setting & did not have enough propellant to try for the 80ms case. Orange color in flame during 20s pulse... boroscope next day revealed more chamber spalling! These are not severe conditions, so don't know why it occurred.																			
190	Thrust cal																			
191	Nominal	1	5/5	50%	325	265			43.93	47.11	1.028	0.121	0.054	2.24	96.87	200.95	202.91	0.232	86.096	
192	Nominal	1	5/5	50%	325	265			44.75	47.91	1.028	0.118	0.055	2.15	95.94	203.09	201.79	0.230	88.107	
193	Nominal	1	5/5	50%	325	265			44.01	47.33	1.028	0.112	0.056	1.99	93.70	207.79	202.84	0.242	86.564	PCIGN was lost during a pressure spike. Reading shift low, but can still continue testing
194	No ignition-Nominal	1	0/10	50%	325	265	-262	-265			1.028									
195	Nominal	1	10/10	50%	325	265	-262	-266	44.04	46.96	1.028	0.111	0.057	1.97	95.39	214.83	202.69	0.213	88.715	
196	Nominal	0.5	5/5	50%	325	265	-262	-264	45.62	49.55	1.028	0.120	0.058	2.06	97.36	206.96	203.55	0.286	43.798	
197	Nominal	0.5	5/5	50%	325	265	-262	-265	46.51	50.02	1.028	0.120	0.057	2.10	96.91	205.84	204.22	0.255	44.630	
198	Nominal	0.5	5/5	50%	325	265	-262	-262	46.06	49.21	1.028	0.117	0.058	2.01	94.73	207.42	204.56	0.230	43.533	
199	Facility abort- Nominal	0.1	0/5	50%	325	265	-261	-263			1.028									
200	Nominal	0.1	5/5	50%	325	265			52.29	56.07	1.028	0.142	0.074	1.93	101.94	205.21	203.77	0.276	9.931	
201	Facility abort- Nominal	0.1	0/10	50%	325	265	-262	-261			1.028									
202	Nominal	0.1	10/10	50%	325	265	-260	-262	55.32	59.02	1.028	0.142	0.076	1.87	108.13	205.09	202.31	0.270	10.808	
203	Facility abort- Nominal	0.1	0/20	50%	325	265	-260	-260			1.028									
204	Nominal	0.1	20/20	50%	325	265			55.77	58.32	1.028	0.144	0.078	1.85	113.39	205.90	202.29	0.186	10.839	Some orange color and sparking observed in plume
205	Nominal	0.1	20/20	50%	325	265			54.55	57.59	1.028	0.139	0.076	1.83	110.05	208.86	207.56	0.221	10.667	Some orange color and sparking observed in plume
206	Thrust cal																			
NEW Columbium Nozzle SN#1																				
	Interim Activity: The SN#3 nozzle was removed, inspection confirmed spalling seen with boroscope. Virgin spare Nozzle SN1 was put on the stand. Pcign transducer was replaced with the more rugged Tabor sensors.																			
3/12/2010	Day Plan: Run at very benign conditions since we don't know what caused damage. No more than 10pulses. Goal is to get some tests at 80ms																			
	End of Day: Lost Pcign on 1st test. Late ignitions triggering aborts… cannot set abort limits any shorter. Methane lag diminishing as train proceeds… could this be a cause of spalling?																			
207	Thrust Cal																			
208	Late ignition - Nominal	0.1	4/5	25%	325	265	-263	-257	35.33	39.59	1.028	0.119	0.065	1.82	68.75	225.70	204.39	0.311	5.969	Late ignition on last pulse
209	Nominal	0.08	1/1	25%	325	265	-264	-258	38.12	42.25	1.028	0.166	0.086	1.94	69.63	200.02	203.64	0.300	0.000	One pulse to check facility timing
210	Late ignition - Nominal	0.08	2/5	25%	325	265	-264	-257	38.17	41.86	1.028	0.151	0.071	2.13	71.57	205.22	206.65	0.269	6.781	Late ignition
211	Nominal	0.08	5/5	25%	325	265	-256	-264	37.87	41.80	1.028	0.139	0.067	2.07	71.43	206.29	212.16	0.286	7.423	We are loosing methane lag by the 3rd pulse.
212	Nominal	0.1	5/5	25%	325	265			42.50	46.58	1.028	0.128	0.071	1.81	80.57	207.83	211.96	0.293	9.069	Repeat earlier test to check methane lag.
213	Thrust cal																			
	Interim Activity: Looked at data, still loosing methane lag. Don't know what is causing. Replace tabor pressure transducer and add higher range transducer to try to catch the problem																			
3/18/2010	Day Plan: Move to warm conditions, operate in 'safe' mode since we still don't know cause. Goal is to get SOME test for milestone progression and see effect of temp on lag																			
	End of Day: There was difficultly with the Pcav abort, the window is so small at these durations that a late ignition (at the tail end of window) may mean Pcav has not met the abort condition. Easiest solution is to shift the abort window 10ms later even though this may overlap the LOX valve closing																			
214	Thrust cal																			
215	Late ignition - Warm	0.1	0/1	25%	370	265	-238	-237												Ignition occurred after abort (in Zone 4)
216	Late ignition - Warm	0.1	4/5	25%	370	265	-238	-236	40.49	44.48	1.029	0.131	0.065	2.00	75.55	218.38	217.71	0.291	8.128	Late ignition
217	Warm	0.08	5/5	25%	370	265	-238	-235	38.48	42.65	1.029	0.136	0.064	2.11	71.09	222.59	221.96	0.304	6.944	Move to 80ms to mimic 3/12/2010 test in terms of hardware temps
218	Late ignition - Warm	0.08	2/5	25%	370	265	-238	-235	38.73	42.52	1.029	0.146	0.067	2.17	70.88	224.09	219.76	0.277	6.294	Late ignition
219	Late ignition - Warm	0.08	1/5	25%	370	265	-238	-235	30.91	33.77	1.029	0.159	0.076	2.10	53.22	224.36	222.08	0.208	0.000	Repeat of last test. Late ignition
220	Late ignition - Warm	0.08	3/5	25%	370	265	-238	-236	41.74	44.70	1.029	0.135	0.068	2.00	75.90	224.47	220.08	0.216	6.899	Late ignition
221	Warm	0.1	5/5	25%	370	265	-238	-236	40.86	44.38	1.029	0.125	0.066	1.91	76.56	224.04	221.09	0.254	8.172	Return to 100ms to look at hardware temp effects (compare with test 216)
222	Late ignition - Warm	0.1	4/5	25%	370	265	-238	-235	43.52	46.80	1.029	0.130	0.066	1.97	81.05	224.30	221.92	0.243	8.284	Late ignition
223	Thrust cal																			
3/23/2010	Day Plan: Move to Cold conditions, still use relatively benign settings to avoid spalling. The methane recirculation pump broke prior to testing. Decided to proceed with test day even though methane will not meet cold condition.																			
	End of Day: Light spalling was found on post-test inspection. Stopped testing to explore potential causes more thoroughly																			
224	Thrust cal																			
225	Late ignition - Cold	0.1	1/5	25%	325	285	-303	-280	27.45	30.80	1.032	0.118	0.064	1.84	36.73	171.47	190.38	0.245		Aborted on the manifold pressures (both)... looks like late ignition
226	Abort -Cold	0.1	1/5	25%	325	285	-305	-280	39.24	42.27	1.032	0.123	0.066	1.87	57.29	175.72	190.37	0.221	2.495	Abort on PFJ (effect sees in previous cold tests)…ignitions also are later in the cold cases. Will lower PFJ abort to 75 and POJ to 140. Also shift Pcav abort to the right
227	Late ignition - Cold	0.1	2/5	25%	325	285	-305	-280	41.46	45.08	1.032	0.169	0.109	1.55	76.12	175.02	189.09	0.259	9.597	Llate ignition, shift Pcav abort. Pressure transient in Methane on 1st pulse, the drop out causes LOX lag.
228	Abort -Cold	0.1	4/5	25%	325	285	-305	-280	43.97	47.46	1.032	0.165	0.089	1.86	82.43	176.12	189.81	0.244	10.433	Abort POJ: Pressure transient in 1st pulse, methane decay is very slow and influction point is more severe (going positive).

					Run Tank Pressure, psig		Run Tank Temperature, Deg F		Thrust paramaters			Average Venturi Mass flow			Chamber pressure	Valve Temps (R)		Test Capsule pressure, psia	Average train Ibit, lbf-s	NOTES
Test #	Test description	Pulse Duration, s	Number of pulses achieved / planned	Duty Cycle	LOX	CH4	LOX	CH4	Thrust (lbf)	Vac Thrust (lbf)	K Factor	LOX Venturi (lbm/s)	CH_4 Venturi (lbm/s)	MR venturi	Pcav (5607)	TOV (5511)	TFV (5011)			
229	Late ignition - Cold	0.08	0/5	25%	325	285	-305	-279										0.329		Late ignition… looks like it ignited on LAST spark or after
230	Late ignition - Cold	0.08	2/5	25%	325	285	-305	-280	38.96	42.83	1.032	0.200	0.137	1.46	72.27	171.63	188.10	0.281	8.742	Abort POJ - late ignition AND preignition on last (3rd pulse)
231	No ignition -Cold	0.08	0/5	25%	325	285	-305	-281								166.74	188.57	0.307		No ignition… the bleeds had been increased on this run, so they are going to back off to previous sets
232	Abort - Cold	0.08	4/5	25%	325	285	-305	-278	41.57	45.64	1.032	0.146	0.087	1.68	80.50	172.36	188.01	0.278	9.112	Abort POJ
233	Thrust cal																			
Installed Unison Exciter																				
	Interim activity: Anaysis of previous test data shows we need longer pulse trains to resolve pulse behavior. No definitive answer on the coating damage. Materials group analysis shows possible Pesting issue. Previously observed methane lag issues do not appear to be a problem.																			
6/3/2010	Day Plan: Run at nominal conditions. Chamber has been clocked to monitor damage locations. Reduce Duty cycle to 5%, run longer pulse trains (10pulses).																			
	End of Day: After facility abort resulting in a long duration (10s) test, we ended testing to check for damage. Good data from 1st two tests. Double pulse phenomena in run 235																			
234	Thrust cal																			
235	Nominal	0.08	10/10	5%	325	285			33.94	38.89	1.019	0.161	0.086	1.88	68.66	219.55	214.62	0.361	5.557	
236	Nominal	0.08	10/10	5%	325	285			36.58	41.71	1.019	0.184	0.086	2.14	71.38	197.41	211.30	0.374	7.607	
237	Faciity abort - Nominal	0.08	0/10	5%	325	285														Engine aborted on pulse 2, but missed a facility abort and the valves did not closed. Had to use E-stop
	Interim activity: Checked facility and engine. Facility had some heat damage from e-stop blow back. Engine had some discoloration on the bell… some blue that we haven't seen before. Boroscope does not indicate any spalling or other damage internal chamber.																			
6/10/2010	Day Plan: Run Warm/Warm, 3 tests at 10pulse train.																			
	End of Day: Got 3 good tests (good temp, no abort) at condition, and one more at higher temp. Did a timing test to see what would take to get a 40ms pulse duration.																			
238	Thrust Cal																			
239	Warm	0.08	10/10	5%	370	265	-239	-236	36.33	40.88	1.026	0.149	0.067	2.24	69.94	231.30	243.79	0.332	5.298	POJ had gain error, readings are off. Fixed before next test. Did not hit temp targets, line traces will be adjusted
240	Warm	0.08	10/10	5%	370	265	-238	-238	37.59	42.62	1.026	0.149	0.076	1.96	73.71	224.41	223.44	0.366	6.371	
241	Late ignition - Warm	0.08	6/10	5%	370	265	-238	-238	37.11	42.14	1.026	0.160	0.078	2.06	72.41	222.42	226.75	0.367	6.385	Late ignition
242	Warm	0.08	10/10	5%	370	265	-238	-236	39.04	43.75	1.026	0.146	0.077	1.90	74.61	222.94	227.15	0.343	6.742	
243	Warm	0.08	10/10	5%	370	265	-238	-237	37.91	42.77	1.026	0.147	0.078	1.90	74.12	223.06	224.99	0.354	6.646	
244	Cold flow to test 40ms timing	0.04	10/10	5%	370	265														40ms timing sucessful, no aborts
245	Thrust cal																			
	Interim activity: Checked data and looked at double pulse phenomena. May be liquid collecting in manifold, then off gasing and reacting (autoignite) in the methane lag period																			
6/15/2010	Day Plan: Cold/Cold with 3 good tests of 10 pulse trains. Methane reciculation pump sill non-operational, so temperatures will likely not reach target																			
	End of Day: First test was warm. Increased bleeds to get colder. Several aborts on POJ, reduced abort limit to 100psi to correct, then 2 good tests. Last test we reduced methane lag to see if effects double pulse.																			
246	Thrust Cal																			
247	Cold	0.08	10/10	5%	325	285	-302	-280	41.39	46.52	1.027	0.171	0.083	2.07	81.75	179.18	208.01	0.374	8.857	
248	Cold	0.08	10/10	5%	325	285	-301	-280	42.48	48.04	1.027	0.160	0.083	1.92	83.87	177.80	203.27	0.405	9.632	Increased bleed to lower temp
249	Abort - Cold	0.08	7/10	5%	325	285	-301	-279	43.02	48.39	1.027	0.165	0.086	1.92	84.13	170.42	197.65	0.391	10.002	Abort POJ -Increased bleed to lower temp
250	Abort - Cold	0.08	6/10	5%	325	285	-300	-278	43.46	48.64	1.027	0.169	0.088	1.93	83.65	171.23	195.67	0.377	9.947	Abort POJ
251	Cold	0.08	10/10	5%	325	285	-301	-278	42.27	47.51	1.027	0.162	0.083	1.95	83.05	174.29	198.75	0.382	9.850	
252	Cold	0.08	5/5	5%	325	285			38.61	43.93	1.027	0.183	0.088	2.09	75.56	179.68	198.93	0.388	8.391	Changed methane lag to see if can eliminate the double pulse. Double pulse still occurred, severity will be examined
253	Thrust Cal																			
	Interim activity:																			
6/17/2010	Day Plan: Longer pulse trains and possibly 40ms pulse duration																			
	End of Day: Successful day																			
254	Thrust Cal																			
255	Late ignition - Nominal	0.08	12/15	5%	325	265	-262	-268	36.81	41.85	1.030	0.146	0.083	1.74	71.18	207.81	207.51	0.368	6.836	Late ignition
256	Nominal	0.08	15/15	5%	325	265	-261	-265	37.40	42.92	1.030	0.137	0.080	1.70	73.67	208.42	209.57	0.402	7.394	
257	Nominal	0.08	20/20	5%	325	265	-260	-268	38.62	44.03	1.030	0.132	0.077	1.72	75.35	208.13	208.30	0.395	7.967	
258	Nominal	0.08	20/20	5%	325	265	-261	-269	38.92	44.22	1.030	0.132	0.078	1.70	76.49	209.43	207.81	0.386	7.699	
259	Nominal	0.08	30/30	5%	325	265	-260	-270	38.97	44.46	1.030	0.132	0.077	1.72	77.31	213.23	208.79	0.400	7.296	20 pulses look consistant and safe, will tried a 30 to match aerojet testing
260	Nominal	0.04	5/5	5%	325	265	-260	-268	25.22	31.15	1.030	0.151	0.081	1.87	50.16	207.29	196.53	0.433	3.265	
261	Nominal	0.04	5/5	5%	325	265	-260	-271	24.81	30.44	1.030	0.155	0.083	1.88	50.43	206.49	195.77	0.410	3.269	
262	Thrust cal																			
Compact Exciter Installed																				
	Interim activity: Installed the compact exciter, Data system recalibrated, new data channels for compact exiciter data signals																			
7/7/2010	Day Plan: Warm/Warm with the compact exciter. Up to 30 pulse cycles. Nominal mixture ratio. 1 test at low MR at conclusion of day. 40 ms pulse train at end																			
	End of Day: Exciter performed well, there were no dropouts or ignition failures. No issues encountered.																			
263	Thrust cal																			
264	Warm	0.08	10/10	5%	370	265	-242	-239	32.44	38.04	1.038	0.145	0.071	2.03	66.15	228.93	237.69	0.408	4.849	
265	Warm	0.08	30/30	5%	370	265	-241	-238	35.63	41.35	1.038	0.132	0.071	1.86	70.59	229.31	233.21	0.417	5.804	
266	Warm	0.08	30/30	5%	370	265	-240	-238	36.51	42.05	1.038	0.124	0.072	1.73	70.95	232.12	229.18	0.404	6.023	
267	Warm	0.08	30/30	5%	370	265	-241	-237	36.48	42.17	1.038	0.127	0.072	1.77	70.29	236.11	227.42	0.415	5.672	

Test #	Test description	Pulse Duration, s	Number of pulses achieved / planned	Duty Cycle	Run Tank Pressure, psig		Run Tank Temperature, Deg F		Thrust paramaters			Average Venturi Mass flow			Chamber pressure	Valve Temps (R)		Test Capsule pressure, psia	Average train Ibit, lbf-s	NOTES
					LOX	CH4	LOX	CH4	Thrust (lbf)	Vac Thrust (lbf)	K Factor	LOX Venturi (lbm/s)	CH_4 Venturi (lbm/s)	MR venturi	Pcav (5607)	TOV (5511)	TFV (5011)			
268	Warm - Low MR	0.08	10/10	5%	330	265	-241	-247	35.24	41.30	1.038	0.136	0.082	1.66	68.42	229.01	218.89	0.441	5.646	Lower O/F to push ignition limits
269	Warm - Low MR	0.08	10/10	5%	330	265	-240	-240	35.40	41.62	1.038	0.148	0.082	1.81	70.66	224.41	220.06	0.453	6.076	Lower O/F repeat
270	Warm	0.04	5/5	5%	370	265	-240	-240	27.40	33.83	1.038	0.157	0.076	2.07	54.67	220.45	208.57	0.468	3.498	40ms pulse duration- Aborts off
271	Warm	0.04	5/5	5%	370	265	-240	-240	29.45	36.04	1.038	0.146	0.076	1.92	58.82	213.18	215.68	0.480	5.536	40ms pulse duration- Aborts off
272	Thrust cal																			
	Interim activity:																			
7/9/2010	Day Plan: Cold/Cold with the compact exciter. Up to 30 pulse cycles. Nominal mixture ratio. 1 test at low MR at conclusion of day. 40 ms pulse train at end																			
	End of Day: Temperature conditions were too warm, but continued testing to prove out exciter. Test 279 almost out of Nitrogen, so we went to 40ms tests instead of repeating low MR. Double pulse observed in almost all 30pulses.																			
273	Thrust Cal																			
274	Late ignition - Cold	0.08	6/10	5%	325	285	-302	-277	35.96	42.11	1.031	0.199	0.089	2.24	70.80	182.45	204.53	0.449	7.714	Late ignition
275	Cold	0.08	10/10	5%	325	285	-302	-278	37.31	43.83	1.031	0.153	0.080	1.90	75.99	180.72	203.75	0.475	8.705	
276	Cold	0.08	30/30	5%	325	285	-303	-278	37.51	43.55	1.031	0.147	0.073	2.03	77.49	185.91	215.37	0.441	8.114	
277	Cold	0.08	10/10	5%	325	285	-302	-277	40.12	46.38	1.031	0.162	0.086	1.89	79.24	174.35	203.26	0.456	9.189	Try to force the CH4 traces on during test to better regulate temp
278	Cold	0.08	30/30	5%	325	285	-302	-278	40.07	46.25	1.031	0.149	0.075	1.98	81.12	182.90	210.80	0.450	8.630	Try to force the CH4 traces on during test to better regulate temp
279	Late ignition - Cold - Low MR	0.08	3/10	5%	290	285	-302	-277	34.44	40.76	1.031	0.195	0.115	1.70	67.87	175.42	196.45	0.460	7.826	Late ignition Try to force the CH4 traces on during test to better regulate temp.
280	No ignition -Cold	0.04	4/5	5%	325	285	-302	-275	23.71	30.12	1.031	0.173	0.097	1.79	44.74	170.22	192.77	0.467	3.810	Non-ignition
281	No ignition -Cold	0.04	3/5	5%	325	285			25.24	31.51	1.031	0.179	0.100	1.80	49.08	169.11	191.70	0.457	4.138	Non-ignition
282	Thrust cal																			
	Interim activity:																			
7/13/2010	Day Plan: Nominal with the compact exciter. Up to 30 pulse cycles. Nominal mixture ratio. 1 test at low MR and a few 40 ms pulse trains																			
	End of Day: Traces left on during all tests to try to maintain temperature better (reduce line heating issues)																			
283	Thrust Cal																			
284	Nominal	0.08	10/10	5%	325	265	-269	-265	34.70	37.99	1.025	0.177	0.077	2.30	69.01	189.04	211.39	0.240	6.853	Traces on during pulses
285	Nominal	0.08	30/30	5%	325	265	-266	-266	38.38	41.95	1.025	0.142	0.067	2.11	78.04	186.62	214.43	0.260	7.706	Traces on during pulses
286	Nominal	0.08	30/30	5%	325	265	-266	-265	40.56	43.95	1.025	0.142	0.069	2.06	80.32	186.30	208.51	0.247	8.088	Traces on during pulses
287	Late ignition -Nominal	0.08	20/30	5%	325	265	-265	-263	36.63	40.36	1.025	0.139	0.079	1.75	71.99	207.68	204.96	0.272	6.063	Late ignition. Traces on during pulses, Adjust Lox trace to get warmer
288	Nominal	0.08	30/30	5%	325	265	-265	-265	38.23	41.94	1.025	0.135	0.073	1.84	75.95	201.92	206.30	0.270	7.382	Traces on during pulses, Repeat…last abort was anomoly- caught PFJ late
289	Nominal	0.04	5/5	5%	325	265	-265	-264	25.56	29.75	1.025	0.149	0.080	1.88	51.92	203.15	196.87	0.305	3.189	Traces on during pulses
290	Late ignition -Nominal - Low MR	0.08	3/30	5%	275	265	-265	-264	32.12	36.36	1.025	0.155	0.099	1.57	65.22	204.27	199.76	0.308	5.465	Late ignition. Traces on during pulses
291	Nominal - Low MR	0.08	30	5%	275	265	-265	-264	30.95	34.71	1.025	0.117	0.077	1.52	62.51	224.61	205.39	0.275	4.341	Traces on during pulses, Warm on LOX
292	Thrust cal																			

REPORT DOCUMENTATION PAGE		Form Approved OMB No. 0704-0188

1. REPORT DATE *(DD-MM-YYYY)*	**2. REPORT TYPE**	**3. DATES COVERED** *(From - To)*
01-06-2012	Technical Memorandum	

4. TITLE AND SUBTITLE
Analysis of 100-lb_f (445-N) LO_2-LCH_4 Reaction Control Engine Impulse Bit Performance

5a. CONTRACT NUMBER

5b. GRANT NUMBER

5c. PROGRAM ELEMENT NUMBER

6. AUTHOR(S)
Marshall, William, M.; Kleinhenz, Julie, E.

5d. PROJECT NUMBER

5e. TASK NUMBER

5f. WORK UNIT NUMBER
WBS 253225.04.02.01.06.01

7. PERFORMING ORGANIZATION NAME(S) AND ADDRESS(ES)
National Aeronautics and Space Administration
John H. Glenn Research Center at Lewis Field
Cleveland, Ohio 44135-3191

8. PERFORMING ORGANIZATION REPORT NUMBER
E-18198

9. SPONSORING/MONITORING AGENCY NAME(S) AND ADDRESS(ES)
National Aeronautics and Space Administration
Washington, DC 20546-0001

10. SPONSORING/MONITOR'S ACRONYM(S)
NASA

11. SPONSORING/MONITORING REPORT NUMBER
NASA/TM-2012-217613

12. DISTRIBUTION/AVAILABILITY STATEMENT
Unclassified-Unlimited
Subject Categories: 12, 20, and 28
Available electronically at http://www.sti.nasa.gov
This publication is available from the NASA Center for AeroSpace Information, 443-757-5802

13. SUPPLEMENTARY NOTES

14. ABSTRACT

Recently, liquid oxygen-liquid methane (LO_2-LCH_4) has been considered as a potential "green" propellant alternative for future exploration missions. The Propulsion and Cryogenic Advanced Development (PCAD) project was tasked by NASA to develop this propulsion combination to enable safe and cost-effective exploration missions. To date, limited experience with such combinations exist, and as a result a comprehensive test program is critical to demonstrating with the viability of implementing such a system. The NASA Glenn Research Center conducted a test program of a 100-lbf (445-N) reaction control engine (RCE) at the Center's Altitude Combustion Stand (ACS), focusing on altitude testing over a wide variety of operational conditions. The ACS facility includes unique propellant conditioning feed systems (PCFS), which allow precise control of propellant inlet conditions to the engine. Engine performance as a result of these inlet conditions was examined extensively during the test program. This paper is a companion to the previous specific impulse testing paper, and discusses the pulsed-mode operation portion of testing, with a focus on minimum impulse bit (MIB) and repeatable pulse performance. The engine successfully demonstrated target MIB performance at all conditions, as well as successful demonstration of repeatable pulse widths. Some anomalous conditions experienced during testing are also discussed, including a double pulse phenomenon, which was not noted in previous test programs for this engine.

15. SUBJECT TERMS
Methane; Liquid oxygen; Propellants; Vacuum; Specific impulse

16. SECURITY CLASSIFICATION OF:			**17. LIMITATION OF ABSTRACT**	**18. NUMBER OF PAGES**	**19a. NAME OF RESPONSIBLE PERSON**
a. REPORT	**b. ABSTRACT**	**c. THIS PAGE**			STI Help Desk (email:help@sti.nasa.gov)
U	U	U	UU	52	**19b. TELEPHONE NUMBER** *(include area code)* 443-757-5802